In the present study, we assessed the oral and nasal FeNO levels in a population of normal subjects, patients with eosinophilic chronic rhinosinusitis (ECRS), and non-eosinophilic CRS (non-ECRS) patients. In Japan, ECRS has been proposed as a subtype of CRS with an intractable clinical course accompanied by the infiltration of numerous activated eosinophils into the paranasal sinus mucosa [11–13]. Eosinophil infiltration is commonly accompanied with histological abnormalities such as fibrosis, thickening of the basement membrane, and epithelial detachment. While the clinical characteristics of ECRS are apparently different from those of non-ECRS, a clear definition that can be used to differentiate each subtype has yet to be established.

We also compared NO production and metabolism pathways of paranasal sinus mucosa between ECRS and non-ECRS patients. The mRNA expressions of three nitric oxide synthase (NOS) isoforms, interleukin-5 (IL-5), and transforming growth factor-beta (TGF-β) were quantitatively analyzed by real-time PCR. The localization of inducible NOS (iNOS) and nitrotyrosine (NT), a marker for oxidized NO metabolites, was immunohistologically examined. There is so far limited information available for FeNO levels in CRS patients in Japan. We found that measurement of oral and nasal FeNO levels was useful in differentiating ECRS from non-ECRS based on the distinctly augmented NO metabolism that underlies ECRS.

2. Patients and methods

2.1. Nitric oxide measurements

Thirty-three ECRS and 16 non-ECRS patients were included in the cross-sectional study of FeNO measurements. Thirty-eight age-matched normal volunteers served as controls. The diagnosis of ECRS was based on clinical symptoms, endoscopic findings, and CT scanning, in accordance with preliminary criteria proposed at the clinical symposium of the 35th Annual Meeting of the Japan Rhinologic Society in 2006 [12]. All patients showed multiple nasal polyps bilaterally, characteristic mucus secretion with high viscosity, and dominant opacification of the ethmoid sinus by CT scanning. Three patients in the non-ECRS group showed a solitary nasal polyp unilaterally without clinical features compatible with ECRS. None of the patients had received topical or systemic steroids for at least 4 weeks before the visit. Patients who had undergone previous sinus surgery were excluded. The CT images were subjected to radiological grading using the Lund-Mackay system [14]. Total sinus scores were calculated bilaterally (range, 0–24). In addition, the E/M ratio (ratio of the averaged ethmoid cells to the maxillary sinus scores) and the PE/AE ratio (ratio of the posterior ethmoid to the anterior ethmoid scores) were calculated as described elsewhere [15].

Oral and nasal FeNO levels were measured before treatment using a handheld electrochemical analyzer (NObreath®, Bedfont Scientific Ltd., Rochester, UK) according to ATS/ERS guidelines [3,16]. For oral FeNO measurements, subjects were advised to exhale for 16 s at a flow rate of 50 mL/s through a mouthpiece. For nasal FeNO measurements, subjects were instructed to exhale transnasally with their mouth closed into a nose adaptor as described elsewhere [17]. Each measurement was performed in triplicate, and the mean value was used for analysis.

2.2. RT-PCR analysis

Ethmoid sinus and nasal polyp specimens were obtained from 18 ECRS and 14 non-ECRS patients who chose surgical therapy and underwent endoscopic sinus surgery. At the time of the surgery, the specimens were divided and either immersed in RNA later™ solution (Ambion, Austin, TX) for real-time RT-PCR, or, alternatively, fixed in 4% paraformaldehyde for immunohistochemistry.

Quantitative PCR analysis was performed on the ABI Prisms 7300 system (Applied Biosystems, Foster City, CA, USA). Cellular RNA was isolated using RNeasy mini kits (Qiagen, Valencia, CA). Total RNA was then reverse-transcribed to cDNA using a High Capacity RNA-to-cDNA kit (Applied Biosystems) according to the instructions supplied by the manufacturer. Gene expression was measured on a real-time PCR system using TaqMan Gene Expression Assays.

PCR primers specific for neuronal NOS (nNOS or NOS1; Hs00167223_m1), iNOS (NOS2; Hs01075529_m1), endothelial NOS (eNOS or NOS3; Hs01574659_m1), IL-5 (Hs00174200_m1), and TGF-β, (Hs99999918_m1) were used. Primers for GAPDH (Hs99999905_m1) were used as a reference. PCR cycles were run in triplicate for each sample. Amplifications of the PCR products were quantified by the number of cycles and the results were analyzed using the comparative cycle threshold (Ct) method ($2^{-\Delta\Delta Ct}$). The Ct values for target genes were normalized to the value of GAPDH by calculating the change in Ct ($^{\Delta}$Ct). Ct values of 34 or higher were considered as the lowest limit of detection. The quantities of target gene expression were presented as relative rates compared with the expression of the reference gene GAPDH (ratio: target gene/GAPDH expression).

2.3. Immunohistochemistry

Primary antibodies used were anti-human iNOS mouse monoclonal antibody (clone 2D2-B2; R&D Systems, Minneapolis, MN) and anti-nitrotyrosine mouse monoclonal antibody (clone 39B6; Santa Cruz, CA). Immunostaining was carried out on 5-μm-thick cryostat sections using mucosal specimens from the same patients as described in RT-RCR. For antigen retrieval, sections were immersed in Histo VT One (Nacalai Tesque, Kyoto, Japan) at 70 °C for 40 min. The slides were then incubated overnight at 4 °C with the primary antibodies. Color development was performed using the streptavidin-biotin amplification technique (ChemMate EnVision kit; Dako, Glostrup, Denmark). Peroxidase activity was visualized by the diaminobenzidine solution. Sections were counterstained with Mayer's hematoxylin. Control specimens developed without the primary antibody were used to verify that nonspecific binding was not detectable. Consecutive sections were stained with hematoxylin-eosin (HE) in order to view the mucosal pathology and to assess the degree of eosinophil infiltration.

We carried out semi-quantitative analysis to compare the immunohistological distribution of NT-positive cells in the submucosal layer between the groups. Cell counts were made in five fields at a magnification of 400 from randomly selected sections blind to the clinical diagnosis. The study protocol was approved by the Institutional Review Board at the Hiroshima University School of Medicine and written informed consent was obtained from all patients..

2.4. Data analysis

For multiple comparisons, screening of data for differences was first carried out using ANOVA. If the analysis gave a significant result, further comparison was done by the Mann–Whitney U test for between-group analysis. Correlation coefficients were calculated by the Spearman method. P values < 0.05 were considered to indicate statistical significance.

3. Results

3.1. Comparison of FeNO levels between non-ECRS and ECRS patients

The clinical characteristics of the study population are summarized in Table 1. A significant difference between the non-ECRS and the ECRS groups was found in the baseline data of

Table 1
Background and baseline characteristics of the study population.

	Non-ECRS patients	ECRS patients
Number	16	33
Age	59.7 (22–74)	57.7 (32–77)
Asthma	0	18**
Blood eosinophils (%)	2.7 (0.2–8.9)	8.5 (2–18)**
CT score	10.3 (4–21)	15.3 (7–24)**
E/M ratio	0.56 (0–1.5)	1.45 (0.75–2)**
PE/AE ratio	0.41 (0–1.25)	0.91 (0.5–1.5)**

Data are shown as mean with ranges in parenthesis.
** $P < 0.01$: significant difference compared with the other group.

proportion of asthma and blood eosinophils. In addition, the ECRS patients showed significantly higher CT scores, E/M ratios, and PE/AE ratios, indicating that opacification of the ethmoid sinus was more severe than that of maxillary sinus in this group.

Fig. 1 shows the values of oral and nasal FeNO at pretreatment in each group. The mean oral FeNO levels were 15.3 ppb in normal subjects, 13.5 ppb in non-ECRS patients, and 47.6 ppb in ECRS patients. The ECRS patients showed significantly higher oral FeNO levels compared to those in the other two groups. The mean nasal FeNO levels were 45.5 ppb in normal subjects, 30.5 ppb in non-ECRS patients, and 53.9 ppb in ECRS patients. Compared with the normal group and ECRS group, the non-ECRS patients showed significantly lower nasal FeNO levels. There was no significant difference in nasal FeNO levels between the control group and the ECRS group. Fig. 2 shows the correlation between blood eosinophils and FeNO levels ECRS patients. We found positive correlations between the blood eosinophil percentage and FeNO levels in ECRS patients, with the coefficient being higher for nasal FeNO than for oral FeNO ($r = 0.604$ vs. $r = 0.309$).

3.2. Real-time RT-PCR analysis

Quantitative real-time PCR was conducted to assess mRNA levels of the three NOS isoforms, IL-5 and TGF-β in the ethmoid sinus mucosa (Fig. 3). The ECRS patients showed significant upregulation of iNOS and IL-5 mRNA expression compared to the

non-ECRS patients. There was no significant difference in eNOS and TGF-β mRNA levels between the groups. As for nNOS mRNA expression, about half of the specimens in both groups were judged as being below the limit of detection. Nasal polyps in the ECRS patients showed profiles similar to ethmoid sinus mucosa in the same subjects, with the latter having higher levels of iNOS and IL-5 mRNA expression.

3.3. Immunohistological findings

As expected, ECRS patients showed intense inflammatory cell infiltration dominated by eosinophils in their ethmoid mucosa and nasal polyps on conventional histological examination. The mean density of eosinophil accumulation in the ethmoid mucosa for the ECRS group was significantly higher than that of the non-ECRS group (103.1 vs. 16.3 cells/HPF, **$P < 0.01$). Figs. 4 and 5 show representative immunohistological images of the distribution of iNOS- and NT-positive cells in the ethmoid sinus mucosa. Positive iNOS immunoreactivity was mainly localized to ciliated epithelial cells, submucosal glands and associated inflammatory cells in both groups. The degree of epithelial iNOS staining appeared identical in both groups. However, patients in the ECRS group tended to reveal strong iNOS staining of inflammatory cells throughout the submucosal area, with eosinophils being predominant.

NT immunoreactivity was detected in the surface epithelium and particularly around inflammatory cells. Intense NT staining was observed in the submucosal layer of ECRS patients (Fig. 4d). Fig. 6 summarizes the density of NT-positive cells in the submucosal layer for each group. The ECRS patients showed significantly higher rates of NT-positive cells compared to the non-ECRS patients (57.8 vs. 17.7 cells/HPF, **$P < 0.01$). We found an intimate relationship between the degree of NT deposition and eosinophil accumulation.

4. Discussion

Based on the accumulation of evidence so far, there is intimate, not yet fully understood, relation between inflammatory conditions and nitric oxide levels in the human nose and paranasal
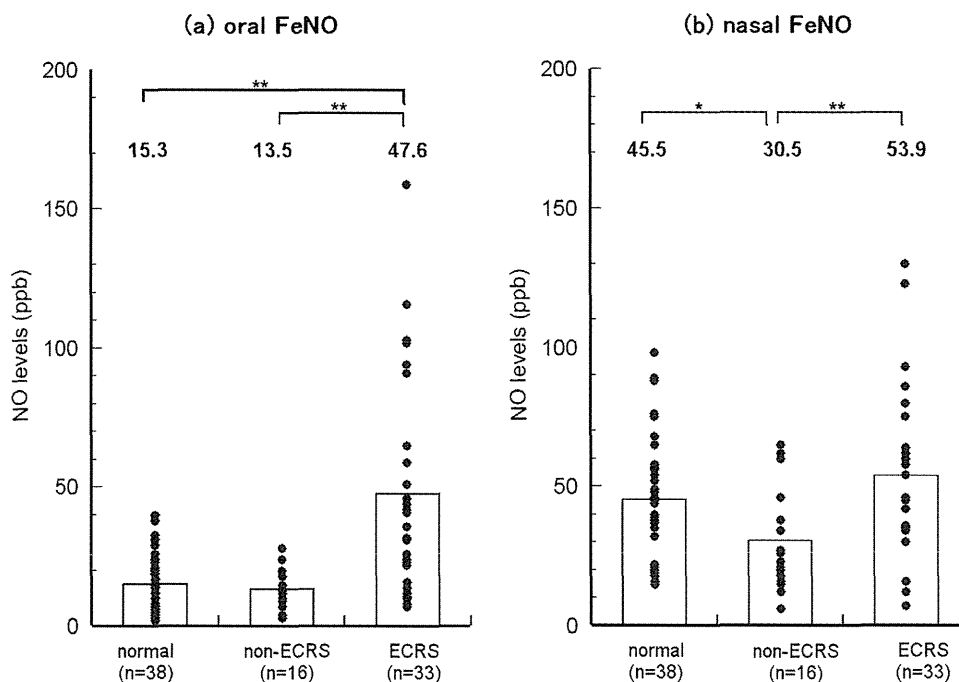

Fig. 1. (a) Oral FeNO and (b) nasal FeNO levels in normal subjects, non-ECRS patients, and ECRS patients. *$P < 0.05$; **$P < 0.01$; FeNO = fractional exhaled nitric oxide.
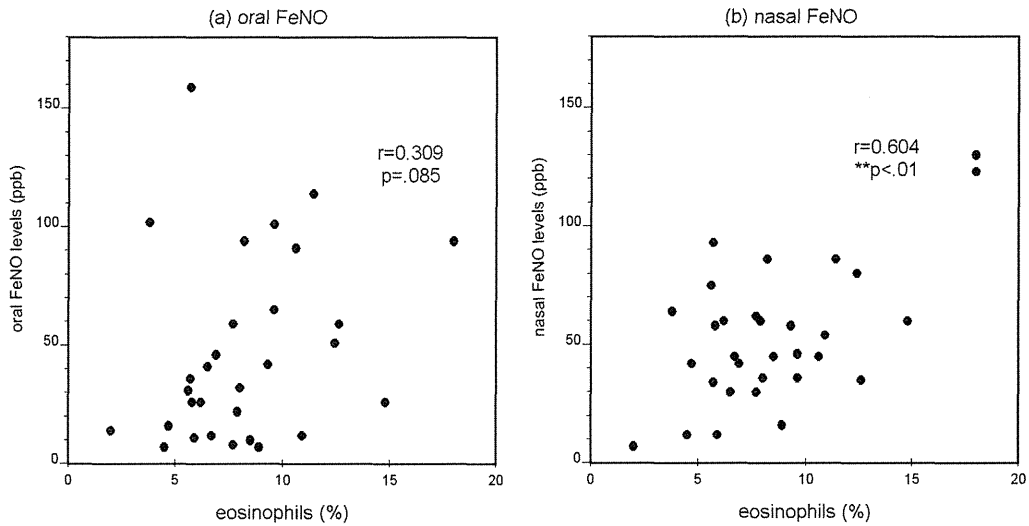
Fig. 2. Correlation between the blood eosinophil percentage and (a) oral FeNO levels and (b) nasal FeNO levels in ECRS patients (n = 33).
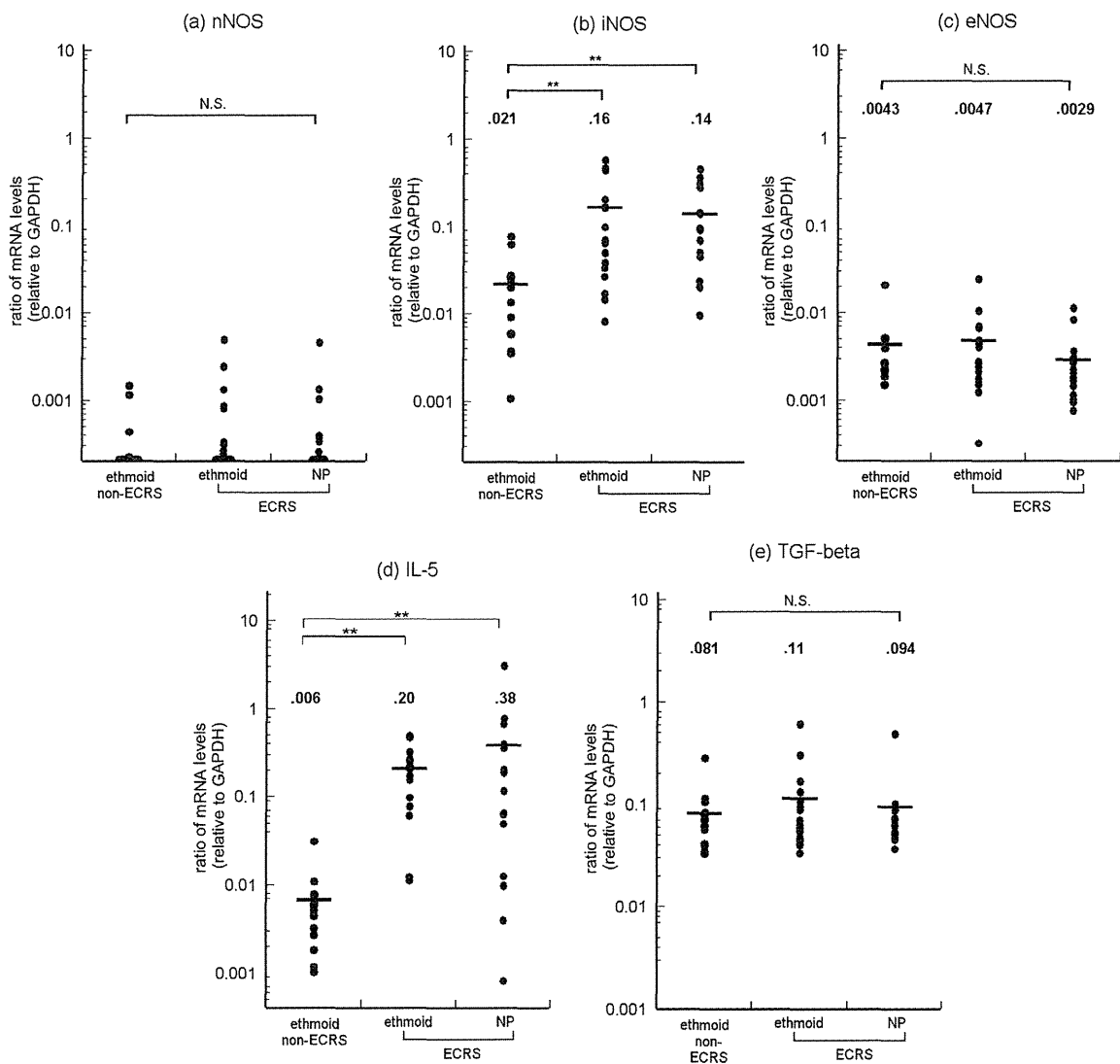

Fig. 3. Comparison of mRNA expression in ethmoid sinus mucosa from non-ECRS and ECRS patients and in nasal polyps from ECRS patients by real-time RT-PCR. The mRNA levels of (a) nNOS (NOS1), (b) iNOS (NOS2), (c) eNOS (NOS3), (d) IL-5, and (e) TGF-β are expressed as ratios relative to GAPDH. Bars indicate mean values. $*P < 0.05$; $**P < 0.01$.
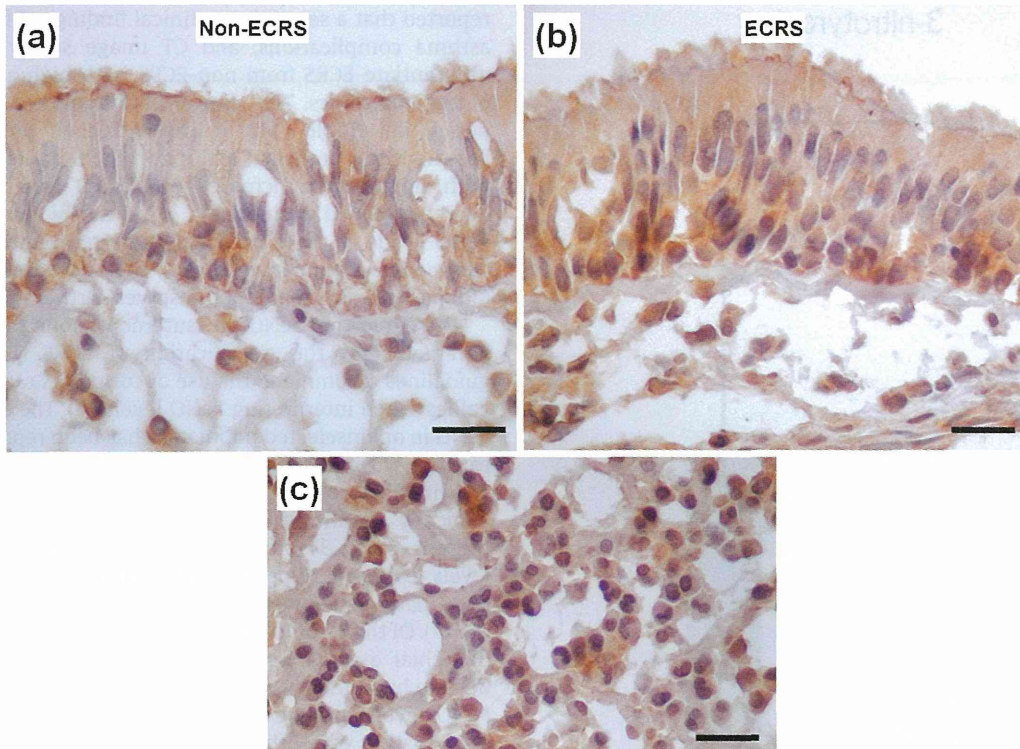
Fig. 4. Immunohistological photographs of iNOS expression in the ethmoid sinus mucosa from (a) a non-ECRS patient and (b) an ECRS patient. (c) Note that iNOS-positive inflammatory cells are scattered predominantly in the submucosal layer of the ECRS patient. Scale bar = 20 μm.
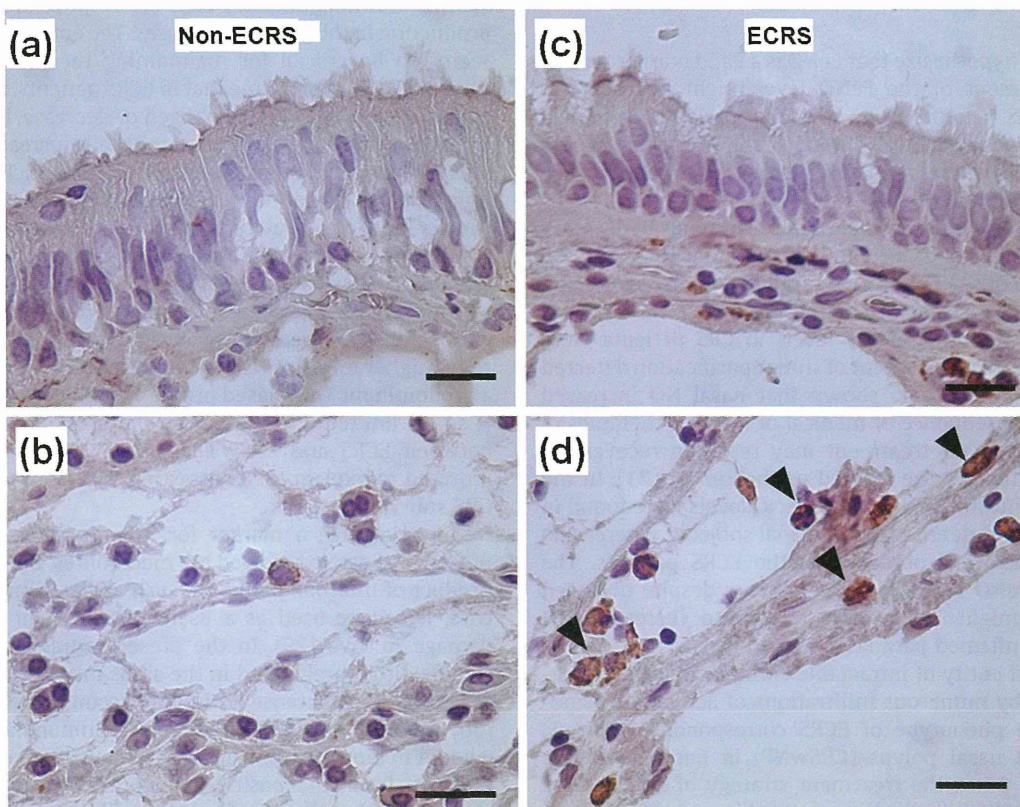

Fig. 5. Immunohistological photographs of 3-nitrotyrosine expression in the ethmoid sinus mucosa from (a and b) a non-ECRS patient and (c and d) an ECRS patient. (d) Note that 3NT-positive inflammatory cells are scattered predominantly in the submucosa of the ECRS patient (arrowheads). Scale bar = 20 μm.
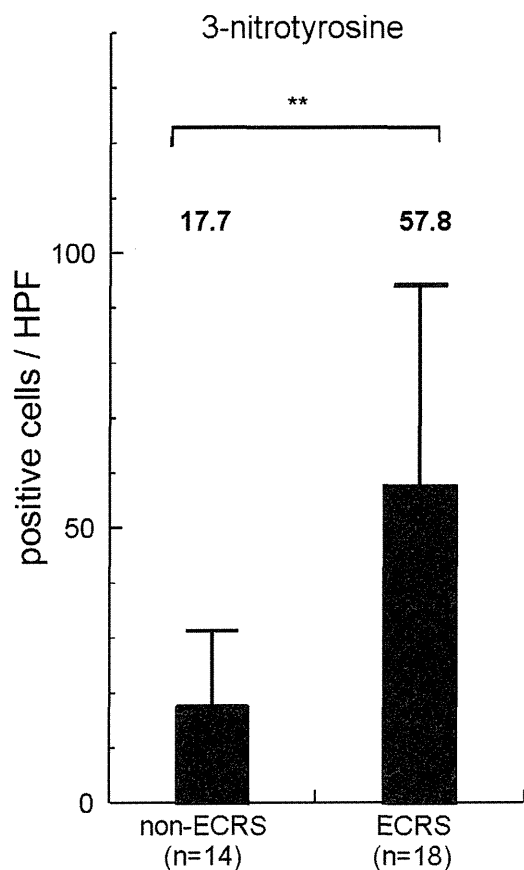
463

3-nitrotyrosine

Fig. 6. Comparison of the density of NT-positive cells in the subepithelial layer of the ethmoid mucosa between the groups. Each column and bar indicates the mean ± SEM. **$P < 0.01$.

sinuses [1,2,9]. We hypothesize that FeNO is a valid marker for CRS and that measurement of the FeNO level might be useful in distinguishing ECRS patients from non-ECRS patients. Relatively high levels of oral and nasal FeNO detected in ECRS patients would reflect the persistence of mucosal eosinophilic inflammation with concomitant upregulation of iNOS mRNA.

Several reports have indicate that nasal FeNO tends to decrease in patients with acute and chronic sinusitis, due to hampered ventilation of gaseous NO through occluded sinus ostia and increased NO absorption by inflamed sinus mucosa [8,18,19]. Arnal et al. [20] reported that nasal NO levels in CRS patients were inversely correlated with the extent of sinus opacification detected on CT scans. It has been also shown that nasal NO increased significantly as a consequence of medical or surgical therapies of CRS, thus suggesting that treatment may result in recovery of normal NO production by the ciliated epithelium [19,21]. In the present study, significantly lower nasal FeNO levels were found in untreated non-ECRS patients than in normal subjects, whereas no significant difference was observed in the ECRS patients. The unchanged nasal FeNO levels in ECRS patients despite occluded sinus ventilation might be in part related to increased NO production in the inflamed paranasal sinus mucosa.

ECRS is a clinical entity of intractable chronic sinus inflammation accompanied by numerous infiltrations of activated eosinophils [11–13]. The phenotype of ECRS corresponds to chronic rhinosinusitis with nasal polyps (CRSwNP) in Europe and the United States [22]. Since the treatment strategy of ECRS differs from that of non-ECRS, diagnostic criteria that can differentiate ECRS from non-ECRS before surgery or that can be used in outpatient clinics are highly desirable. Recently, Sakuma et al. [15]

reported that a set of three clinical findings of blood eosinophilia, asthma complications, and CT image score assessment could differentiate ECRS from non-ECRS with high accuracy in regular outpatient clinics. The clinical background of the present study population (Table 1) is in line with their proposal. The higher prevalence of bronchial asthma in ECRS patients was associated with significantly increased oral FeNO levels. In addition, the degree of blood eosinophilia significantly correlated with nasal FeNO levels in these patients. The interpretation of the relation between upper and lower airway function based on FeNO levels in CRS patients is a topic that deserves further attention [20,23].

We agree that FeNO measurement alone cannot be a definite parameter for the classification of ECRS. The 2011 ATS/ERS guidelines recommend the use of cut points rather than reference values when interpreting FeNO levels [4]. The distribution of oral FeNO in an unselected population has been reported to be skewed to the right and the upper limit of "normal" ranges from 27 to 57 ppb. Shaw et al. proposed that the optimum cut point for a clinically significant oral FeNO was set as 26 ppb [24]. In the present study, 31 out of 38 normal subjects showed oral FeNO levels less than 26 ppb (specificity rate 81.5%), and 22 out of 33 ECRS patients showed levels more than 26 ppb (sensitivity rate 66.6%). Of the 22 ECRS patients, 14 patients had a clinical history of bronchial asthma but 8 patients had no asthmatic symptoms despite high oral FeNO levels. Based on the results, we argue that FeNO levels may be used to support the diagnosis of ECRS in combination with other subjective and objective factors.

ECRS patients showed increased iNOS and IL-5 mRNA expression as compared with non-ECRS patients. On the other hand, mRNA levels for constitutive NOS isoforms appeared to be unchanged. It is well known that iNOS expression is stimulated by pro-inflammatory mediators and bacterial products such as lipopolysaccharides. The immunohistological results indicate that iNOS activities both by the ciliary epithelium and by the submucosal inflammatory cells are responsible for dominant NO production in the paranasal sinuses. The epithelial iNOS expression seems to be crucial for maintaining the mucociliary clearance system [5,25]. We assume that in ECRS patients, iNOS expression in epithelial cells may be unchanged or decrease, but NO production by iNOS derived from inflammatory cells increases significantly. It should be noted that excess secretions and thick aqueous mucosal lining by inflammation may inhibit diffusion of gaseous NO into the air-filled nasal cavity, similar to the case in suppurative lung conditions [26]. No significant difference in TGF-β mRNA levels was observed between the groups. TGF-β plays a pivotal role in the airway remodeling process through promoting the synthesis of extracellular matrices. In western countries, patients with CRSsNP show higher levels of TGF-β, whereas CRSwNP is characterized by a predominant Th2-biased profile with high IL-5 levels [27]. There is so far limited information on the cytokine expression pattern between ECRS and CRSwNP patients [28]. Further studies are required to explain the contrasting TGF-β expression among the CRS subtypes in Japan.

Nitrotyrosine, a marker for inflammation, is formed in the presence of active oxidized NO metabolites. Because NT is a stable product of multiple pathways such as the formation of peroxynitrite, it can be used as a useful determinant of NO-dependent damage in vivo [29]. In the present study, NT expression was significantly upregulated in the sinus mucosa from ECRS patients associated with intense eosinophil accumulation. Bernardes et al. [30] reported that NT staining was immunohistologically more evident in biopsies from sinusitis patients than in healthy mucosa. They also found that positive NT expression was largely confined to eosinophils in the area featuring epithelial disruption. Naraghi et al. [25] reported that NO metabolite levels of sinus lavage fluid in CRS patients were significantly higher than those in healthy

subjects. These results, together with ours, suggest that in ECRS patients, the formation of NT can be related to the autotoxic NO mechanism, similar to the case with bronchial asthma [31].

In conclusion, the present study validates the role of oral and nasal FeNO measurements as a parameter for the classification and definition of different CRS subtypes in Japan. We consider that higher FeNO levels in ECRS patients closely correlate with augmented iNOS expression and are accompanied by the excretion of NO metabolites into the paranasal sinus mucosa. Further accumulation of a consensus regarding the standardization of reliable measurements and the possibility of using FeNO to monitor therapeutic effects would be desirable.

Conflict of interest

None of the authors have any conflict of interest to declare in relation to this study.

Acknowledgments

References

[1] Lundberg JO, Weitzberg E. Nasal nitric oxide in man. Thorax 1999;54:947–52.

[2] Scadding G. Nitric oxide in the airways. Curr Opin Otolaryngol Head Neck Surg 2007;15:258–63.

[3] American Thoracic Society, European Respiratory Society. ATS/ERS recommendations for standardized procedures for the online and offline measurement of exhaled lower respiratory nitric oxide and nasal nitric oxide, 2005. Am J Respir Crit Care Med 2005;171:912–30.

[4] Dweik RA, Boggs PB, Erzurum SC, Irvin CG, Leigh MW, Lundberg JO, et al. An official ATS clinical practice guideline: interpretation of exhaled nitric oxide levels (FENO) for clinical applications. Am J Respir Crit Care Med 2011;184:602–15.

[5] Lundberg JO, Farkas-Szallasi T, Weitzberg E, Rinder J, Lidholm J, Anggaard A, et al. High nitric oxide production in human paranasal sinuses. Nat Med 1995;1:370–3.

[6] Barnes PJ, Dweik RA, Gelb AF, Gibson PG, George SC, Grasemann H, et al. Exhaled nitric oxide in pulmonary diseases: a comprehensive review. Chest 2010;138:682–92.

[7] Sahin G, Klimek L, Mullol J, Hörmann K, Walther LE, Pfaar O. Nitric oxide: a promising methodological approach in airway diseases. Int Arch Allergy Immunol 2011;156:352–61.

[8] Lindberg S, Cervin A, Runer T. Nitric oxide production in the upper airways is decreased in chronic sinusitis. Acta Otolaryngol (Stockh) 1997;117:113–7.

[9] Maniscalco M, Sofia M, Pelaia G. Nitric oxide in upper airways inflammatory diseases. Inflamm Res 2007;56:58–69.

[10] Guida G, Rolla G, Badiu I, Marsico P, Pizzimenti S, Bommarito L, et al. Determinants of exhaled nitric oxide in chronic rhinosinusitis. Chest 2010;137:658–64.

[11] Haruna S, Otori N, Moriyama H, Nakanishi M. Olfactory dysfunction in sinusitis with infiltration of numerous activated eosinophils. Auris Nasus Larynx 2006;33:23–30.

[12] Takeno S, Hirakawa K, Ishino T. Pathological mechanisms and clinical features of eosinophilic chronic rhinosinusitis in the Japanese population. Allergol Int 2010;59:247–56.

[13] Nakayama T, Yoshikawa M, Asaka D, Okushi T, Matsuwaki Y, Otori N, et al. Mucosal eosinophilia and recurrence of nasal polyps – new classification of chronic rhinosinusitis. Rhinology 2011;49:392–6.

[14] Lund VJ, Mackay IS. Staging in rhinosinusitus. Rhinology 1993;31:183–4.

[15] Sakuma Y, Ishitoya J, Komatsu M, Shiono O, Hirama M, Yamashita Y, et al. New clinical diagnostic criteria for eosinophilic chronic rhinosinusitis. Auris Nasus Larynx 2011;38:583–8.

[16] Antus B, Horvath I, Barta I. Assessment of exhaled nitric oxide by a new hand-held device. Respir Med 2010;104:1377–80.

[17] Takeno S, Noda N, Hirakawa K. Measurements of nasal fractional exhaled nitric oxide with a hand-held device in patients with allergic rhinitis: relation to cedar pollen dispersion and laser surgery. Allergol Int 2011;61:93–100.

[18] Weschta M, Deutschle T, Riechelmann H. Nasal fractional exhaled nitric oxide analysis with a novel hand-held device. Rhinology 2008;46:23–7.

[19] Ragab SM, Lund VJ, Saleh HA, Scadding G. Nasal nitric oxide in objective evaluation of chronic rhinosinusitis therapy. Allergy 2006;61:717–24.

[20] Arnal JF, Flores P, Rami J, Murris-Espin M, Bremont F, Pasto I, et al. Nasal nitric oxide concentration in paranasal sinus inflammatory diseases. Eur Respir J 1999;13:307–12.

[21] Noda N, Takeno S, Fukuiri T, Hirakawa K. Monitoring of oral and nasal exhaled nitric oxide in eosinophilic chronic rhinosinusitis: a prospective study. Am J Rhinol Allergy 2012;26:255–9.

[22] Meltzer EO, Hamilos DL, Hadley JA, Lanza DC, Marple BF, Nicklas RA, et al. Rhinosinusitis: developing guidance for clinical trials. J Allergy Clin Immunol 2006;118:S17–61.

[23] Galli J, Montuschi P, Passàli GC, Laruffa M, Parrilla C, Paludetti G. Exhaled nitric oxide measurement in patients affected by nasal polyposis. Otolaryngol Head Neck Surg 2012;147:351–6.

[24] Shaw DE, Berry MA, Thomas M, Green RH, Brightling CE, Wardlaw AJ, et al. The use of exhaled nitric oxide to guide asthma management: a randomized controlled trial. Am J Respir Crit Care Med 2007;176:231–7.

[25] Naraghi M, Deroee AF, Ebrahimkhani M, Kiani S, Dehpour A. Nitric oxide: a new concept in chronic sinusitis pathogenesis. Am J Otolaryngol 2007;28:334–7.

[26] Ho LP, Innes JA, Greening AP. Nitrite levels in breath condensate of patients with cystic fibrosis is elevated in contrast to exhaled nitric oxide. Thorax 1998;53:680–4.

[27] Van Crombruggen K, Zhang N, Gevaert P, Tomassen P, Bachert C. Pathogenesis of chronic rhinosinusitis: inflammation. J Allergy Clin Immunol 2011;128:728–32.

[28] Sejima T, Holtappels G, Kikuchi H, Imayoshi S, Ichimura K, Bachert C. Cytokine profiles in Japanese patients with chronic rhinosinusitis. Allergol Int 2012;61:115–22.

[29] Kang BH, Huang NC, Wang HW. Possible involvement of nitric oxide and peroxynitrite in nasal polyposis. Am J Rhinol 2004;18:191–6.

[30] Bernardes JF, Shan J, Tewfik M, Hamid Q, Frenkiel S, Eidelman DH. Protein nitration in chronic sinusitis and nasal polyposis: role of eosinophils. Otolaryngol Head Neck Surg 2004;131:696–703.

[31] Berry MA, Shaw DE, Green RH, Brightling CE, Wardlaw AJ, Pavord ID. The use of exhaled nitric oxide concentration to identify eosinophilic airway inflammation: an observational study in adults with asthma. Clin Exp Allergy 2005;35:1175–9.

RESPIRATORY
RESEARCH

RESEARCH   Open Access

Pseudomonas aeruginosa elastase causes transient disruption of tight junctions and downregulation of PAR-2 in human nasal epithelial cells

Kazuaki Nomura[1,2], Kazufumi Obata[1], Takashi Keira[1,2], Ryo Miyata[1,4], Satoshi Hirakawa[3], Ken-ichi Takano[1], Takayuki Kohno[4], Norimasa Sawada[2], Tetsuo Himi[1] and Takashi Kojima[4*]

Abstract

Background: *Pseudomonas aeruginosa* causes chronic respiratory disease, and the elastase enzyme that it produces increases the permeability of airway epithelial cells owing to the disruption of tight junctions. *P. aeruginosa* is also implicated in prolonged chronic rhinosinusitis. However, the effects of *P. aeruginosa* elastase (PE) against the barrier formed by human nasal epithelial cells (HNECs) remain unknown.

Methods: To investigate the mechanisms involved in the disruption of tight junctions by PE in HNECs, primary cultures of HNECs transfected with human telomerase reverse transcriptase (hTERT-HNECs) were used. The hTERT-HNECs were pretreated with inhibitors of various signal transduction pathways, PKC, MAPK, p38MAPK, PI3K, JNK, NF-κB, EGF receptor, proteasome, COX1 and COX2 before treatment with PE. Some cells were pretreated with siRNA and agonist of protease activated receptor-2 (PAR-2) before treatment with PE. Expression and structures of tight junctions were determined by Western blotting, real-time PCR, immunostaining and freeze-fracture. Transepithelial electrical resistance (TER) was examined as the epithelial barrier function.

Results: PE treatment transiently disrupted the epithelial barrier and downregulated the transmembrane proteins claudin-1 and -4, occludin, and tricellulin, but not the scaffold PDZ-expression proteins ZO-1 and -2 and adherens junction proteins E-cadherin and β-catenin. The transient downregulation of tight junction proteins was controlled via distinct signal transduction pathways such as the PKC, MAPK, PI3K, p38 MAPK, JNK, COX-1 and -2, and NF-κB pathways. Furthermore, treatment with PE transiently decreased PAR-2 expression, which also regulated the expression of the tight junction proteins. Treatment with a PAR-2 agonist prevented the downregulation of the tight junction proteins after PE treatment in HNECs.

Conclusions: PE transiently disrupts tight junctions in HNECs and downregulates PAR-2. The transient disruption of tight junctions by PE might occur repeatedly during chronic rhinosinusitis.

Keywords: *Pseudomonas aeruginosa* elastase, Tight junctions, Barrier function, Human nasal epithelial cells, Signal transduction, PAR-2

* Correspondence: ktakashi@sapmed.ac.jp
[4]Department of Cell Science, Research Institute for Frontier Medicine,
Sapporo Medical University School of Medicine, South-1, West-17, Chuo-ku,
Sapporo 060-8556, Japan
Full list of author information is available at the end of the article

BioMed Central

Introduction

Pseudomonas aeruginosa (*P. aeruginosa*) is a virulent Gram-negative bacterium that causes aggressive infections in patients compromised by pre-existing respiratory disease such as cystic fibrosis and diffuse panbronchiolitis [1,2]. *P. aeruginosa* is also associated with prolonged chronic rhinosinusitis (CRS) [3].

P. aeruginosa secretes several virulence factors such as exotoxin A, exoenzyme S, pyocyanin, and elastase, which play an important role in pathogenesis [4,5]. *P. aeruginosa* elastase (PE) increases paracellular permeability in lung epithelial cells via mechanisms involving tight junction disruption and cytoskeletal reorganization [6]. PE affects epithelial cells via multiple mediators of signaling including activation of PKC, EGFR, ERK1/2, NF-κB, urokinase/uPAR, and protease activated receptor-2 (PAR-2) [1,2,7-11]. PKC signaling is involved in PE-induced epithelial barrier disruption via tight junction translocation and cytoskeletal reorganization in the human bronchial adenocarcinoma cell line Calu-3 [2].

PE disables PAR-2 in respiratory epithelial cells [1]. Protease-activated receptors (PARs) are G protein-coupled receptors with seven transmembrane domains, which are cleaved at an activation site within the N-terminal exodomain by a variety of proteases [1]. Four PARs (PAR-1, -2, -3, and -4) have been identified and are widely expressed by cells in blood vessels, connective tissue, leukocytes, epithelium, and many airway cells [12]. PAR-2 is expressed in airway epithelium, and its activation initiates multiple effects including enhanced airway inflammation and reactivity [13]. Upregulation of PAR-2 is observed in the respiratory epithelium of patients with asthma and chronic rhinosinusitis [14,15]. PAR-2 activation also affects the airway epithelial barrier [16]. However, details of the mechanistic effects of PE against the epithelial barrier via PAR-2 remain unknown.

Airway epithelium of human nasal mucosa acts as a physical barrier that protects against inhaled substances and pathogens because of its tight junctions, the most apical intercellular junctions [17-19]. Tight junctions are formed by not only the integral membrane proteins claudins, occludin, tricellulin, and junctional adhesion molecules (JAMs), but also by many peripheral membrane proteins, including the scaffold PDZ-expression proteins zonula occludens (ZO) and non-PDZ-expressing proteins [20-23]. We previously reported that, in HNECs *in vivo*, the tight junction molecules occludin, tricellulin, JAM-A, claudin-1, -4, -7, -8, -12, -13, and -14, and ZO-1 and -2 were detected together with well-developed tight junction strands [17,24,25]. The tight junctions and the well-developed barrier function in primary *in vitro* cultures of HNECs transfected with human telomerase reverse transcriptase (hTERT-HNECs) were very similar to those observed in HNECs *in vivo* [24-27]. Furthermore, in the *in vitro* HNECs, tight junction molecules and barrier function are upregulated by various stimuli via distinct signal transduction pathways [25].

In the present study, to investigate the effects of elastase on the tight junction barrier of HNECs, hTERT-HNECs were treated with PE. Treatment with PE transiently disrupted the epithelial barrier and downregulated the transmembrane proteins claudin-1 and -4, occludin, and tricellulin but not the scaffold PDZ-expression proteins ZO-1 and -2 and adherens junction proteins E-cadherin and β-catenin. Downregulation of tight junction proteins because of PE treatment was mediated via distinct signal transduction pathways. Furthermore, treatment with PE transiently decreased PAR-2 expression, which partially regulated the expression of the tight junction proteins. A PAR-2 agonist prevented the downregulation of tight junction proteins after PE treatment in HNECs.

Materials and methods

Reagents

A pan-PKC inhibitor (GF109203X), MEK1/2 inhibitor (U0126), p38 MAPK inhibitor (SB203580), and PI3K inhibitor (LY294002) were purchased from Calbiochem-Novabiochem Corporation (San Diego, CA). JNK inhibitor (SP600125) and NF-κB inhibitor (IMD-0354) were purchased from Sigma-Aldrich (St. Louis, MO). Epidermal growth factor (EGF) receptor inhibitor (AG1478) was purchased from Calbiochem-Novabiochem Corporation (San Diego, CA). Proteasome inhibitor (MG132), the COX1 inhibitor (FR122047), and COX2 inhibitor were purchased from Calbiochem Novabiochem Corporation (San Diego, CA). *Pseudomonas aeruginosa* elastase and neutrophil elastase were purchased from Elastin Products Company, Inc. (Owensville, USA). Protease activated receptor 2 (PAR-2) agonist (*SLIGKV*-NH2) was purchased from R&D Systems, Inc. (Minneapolis, MN). Alexa 488 (green)- and Alexa 594 (red)-conjugated anti-mouse and anti-rabbit IgG antibodies were purchased from Invitrogen. HRP-conjugated polyclonal goat anti-rabbit immunoglobulins were purchased from Dako A/S (Glostrup, Denmark). The ECL Western blotting system was obtained from GE Healthcare UK, Ltd. (Buckinghamshire, UK).

Cell culture and treatments

The cultured HNECs were derived from the mucosal tissues of patients who underwent inferior turbinectomy at the Sapporo Hospital of Hokkaido Railway Company and the KKR Sapporo Medical Center Tonan Hospital. Informed consent was obtained from all patients and this study was approved by the ethical committees of Sapporo Medical University, the Sapporo Hospital of Hokkaido Railway Company, and the KKR Sapporo Medical Center Tonan Hospital.

The procedures for primary culture of human nasal epithelial cells were as reported previously [26]. Primary cultured HNECs were transfected with the catalytic component of telomerase, the human catalytic subunit of the telomerase reverse transcriptase (hTERT) gene as described previously [26]. The cells were plated on 35-mm or 60-mm culture dishes (Corning Glass Works, Corning, NY, USA), which were coated with rat tail collagen (500 μg of dried tendon/ml 0.1% acetic acid). The cells were cultured in serum-free bronchial epithelial cell basal medium (BEBM, Lonza Walkersville, Inc.; Walkersville, MD, USA) supplemented with bovine pituitary extract (1% v/v), 5 μg/ml insulin, 0.5 μg/ml hydrocortisone, 50 μg/ml gentamycin, 50 μg/ml amphotericin B, 0.1 ng/ml retinoic acid, 10 μg/ml transferrin, 6.5 μg/ml triiodothyronine, 0.5 μg/ml epinephrine, 0.5 ng/ml epidermal growth factor (Lonza Walkersville, Inc.), 100 U/ml penicillin and 100 μg/ml streptomycin (Sigma-Aldrich) and incubated in a humidifier, 5% CO_2:95% air incubator at 37°C. This experiment used cells in the second and third passage. The hTERT-HNECs were treated with 0.1 U (a unit of 3.83 μg/ml) *Pseudomonas aeruginosa* elastase (PE) or 0.01 U (a unit of 1.25 μg/ml) neutrophil elastase (NE). Some cells were pretreated with or without inhibitors of pan-PKC, MEK1/2, p38MAPK, PI3K, JNK, NF-κB, EGF receptor, proteasome, COX1, COX2 and PAR-2 agonist 30 min before treatment with 0.1 U PE. The concentrations of the various inhibitors were used following our previous reports [28,29].

Transfection with small interfering RNA (siRNA)

siRNA duplex oligonucleotides against human PAR 2 (sc-36188) were synthesized by Santa Cruz Biotechnology, inc. (Santa Cruz, CA). The hTERT-transfected HNECs at 24 h after plating were transfected with 100 nM siRNA of PAR-2 using Lipofectamine™ RNAiMAX Reagent (Invitrogen). Some cells were treated with 0.1 U PE after transfection with 100 nM siRNS of PAR-2 for 48 h.

RNA isolation, RT-PCR, and real-time RT-PCR analysis

Total RNA was extracted and purified from hTERT-transfected HNECs using TRIzol reagent (Invitrogen). One microgram of total RNA was reverse transcribed into cDNA using a mixture of oligo(dT) and Superscript II RTase using the recommended conditions (Invitrogen). Each cDNA synthesis was performed in a total volume of 20 μl for 50 min at 42°C and terminated by incubation for 15 min at 70°C. PCR containing 100 pM primer pairs and 1.0 μl of the 20 μl total RT reaction was performed in 20 μl of 10 mM Tris–HCl (pH 8.3), 50 mM KCl, 1.5 mM $MgCl_2$, 0.4 mM dNTPs, and 0.5 U of Taq DNA polymerase (Takara Bio, Inc.; Shiga, Japan), employing 25, 30, or 35 cycles with cycle times of 15 s at 96°C, 30 s at 55°C, and 60 s at 72°C. The final elongation step was 7 min at 72°C. Nine microliters of the 20 μl total PCR reaction was analyzed by gel electrophoresis with 2% agarose after staining with ethidium bromide. To provide a quantitative control for reaction efficiency, PCR reactions were performed with primers coding for the housekeeping gene glyceraldehyde-3-phosphate dehydrogenase (G3PDH). Primers used to detect G3PDH, occludin, tricellulin, claudin-1, -4, -7, PAR-1, and -2 are indicated in Table 1.

Real-time PCR detection was performed using a TaqMan Gene Expression Assay kit with a StepOnePlus™ real-time PCR system (Applied Biosystems; Foster City, CA, USA). The amount of 18S ribosomal RNA (rRNA) (Hs99999901) in each sample was used to standardize the quantity of the following mRNAs: tricellulin (Hs00930631), claudin-1 (Hs00221623), claudin-4 (Hs00533616), claudin-7 (Hs00154575), occludin (Hs00170162).

The relative mRNA expression levels between the control and treated samples were calculated by the difference of the threshold cycle (comparative C_T [$\Delta\Delta C_T$] method) and presented as the average of triplicate experiments with a 95% confidence interval.

Western blot analysis

The hTERT-transfected HNECs were scraped from a 60 mm dish containing 300 μl of buffer (1 mM $NaHCO_3$ and 2 mM phenylmethylsulfonyl fluoride), collected in microcentrifuge tubes, and then sonicated for 10 s. The protein concentrations of the samples were determined using a BCA protein assay reagent kit (Pierce Chemical Co.; Rockford, IL, USA). Aliquots of 15 μl of protein/lane

Table 1 Primers for RT-PCR

Gene	Forward primer	Reverse primer	Product size (bp)
G3PDH	ACCACAGTCCATGCCATCAC	TCCACCACCCTGTTGCTGTA	452
PAR-1	GGATATTTGACCAGCTCCTGG	AGATGGCCAGACAAGTGAAGG	400
PAR-2	CTGCATCTGTCCTCACTGGAA	ATTGCCAGGGAGATGCCAATG	400
Claudin-1	GCTGCTGGGTTTCATCCTG	CACATAGTCTTTCCCACTAGAAG	619
Claudin-4	AGCCTTCCAGGTCCTCAACT	AGCAGCGAGTAGAAG	249
Claudin-7	AGGCATAATTTTCATCGTGG	GAGTTGGACTTAGGGTAAGAGCG	252
Occludin	TCAGGGAATATCCACCTATCACTTCAG	CATCAGCAGCAGCCATGTACTCTTCAC	189
Tricellulin	AGGCAGCTCGGAGACATAGA	TCACAGGGTATTTTGCCACA	200

for each sample were separated by electrophoresis in 5–20% SDS polyacrylamide gels (Daiichi Pure Chemicals Co.; Tokyo, Japan), and electrophoretic transfer to a nitrocellulose membrane (Immobilon; Millipore Co.; Bedford, UK) was performed.

The membrane was saturated for 30 min at room temperature with blocking buffer (25 mM Tris, pH 8.0, 125 mM NaCl, 0.1% Tween 20, and 4% skim milk) and incubated with anti-claudin-1, -4, and -7 anti-occludin, anti-tricellulin, anti-ZO-1, and -2, anti-β-catenin, anti-E-cadherin, anti-actin and anti-PAR-2 antibodies (Table 2) at room temperature for 1 h. The membrane was incubated with HRP-conjugated anti-mouse and anti-rabbit IgG antibodies at room temperature for 1 h. The immuno-reactive bands were detected using an ECL Western blotting system.

Immunocytochemical staining

The hTERT-transfected HNECs grown in 35-mm glass-coated wells (Iwaki, Chiba, Japan), were fixed with cold acetone and ethanol (1:1) at −20°C for 10 min. After rinsing in PBS, the cells were incubated with anti-occludin and anti-claudin-1 antibodies (Table 2) at room temperature for 1 h. Alexa Fluor 488 (green)-conjugated anti-rabbit IgG and Alexa Fluor 592 (red)-conjugated anti-mouse IgG (Invitrogen) were used as secondary antibodies. The specimens were examined using a confocal laser scanning microscope (LSM510; Carl Zeiss, Jena, Germany).

Freeze-fracture analysis

For the freeze-fracture technique, the cells were immersed in 40% glycerin solution after fixation in 2.5% glutaralde-hyde/0.1 M phosphate-buffered saline (PBS). The specimens were fractured at −150°C to −160°C in a JFD-7000 freeze-fracture device (JEOL, Ltd., Tokyo, Japan) and replicated by deposition of platinum/carbon from an electron beam gun positioned at a 45° angle followed by carbon applied from overhead. Replicas were examined at 100kV with a JEM transmission electron microscope (JEOL Ltd., Tokyo, Japan).

Continuous online measurements of transepithelial electrical resistance (TER)

Cells were cultured to confluence on the inner chambers of 12-mm Transwell 0.4-μm pore-size filters (Corning Life Science). Transepithelial electrical resistance (TER) was monitored using a cellZscope (nanoAnalytics, Germany), a computer controlled automated multi-well device (12 wells). The values are expressed in standard units of ohms per square centimeter and presented as the mean ± SD of triplicate experiments.
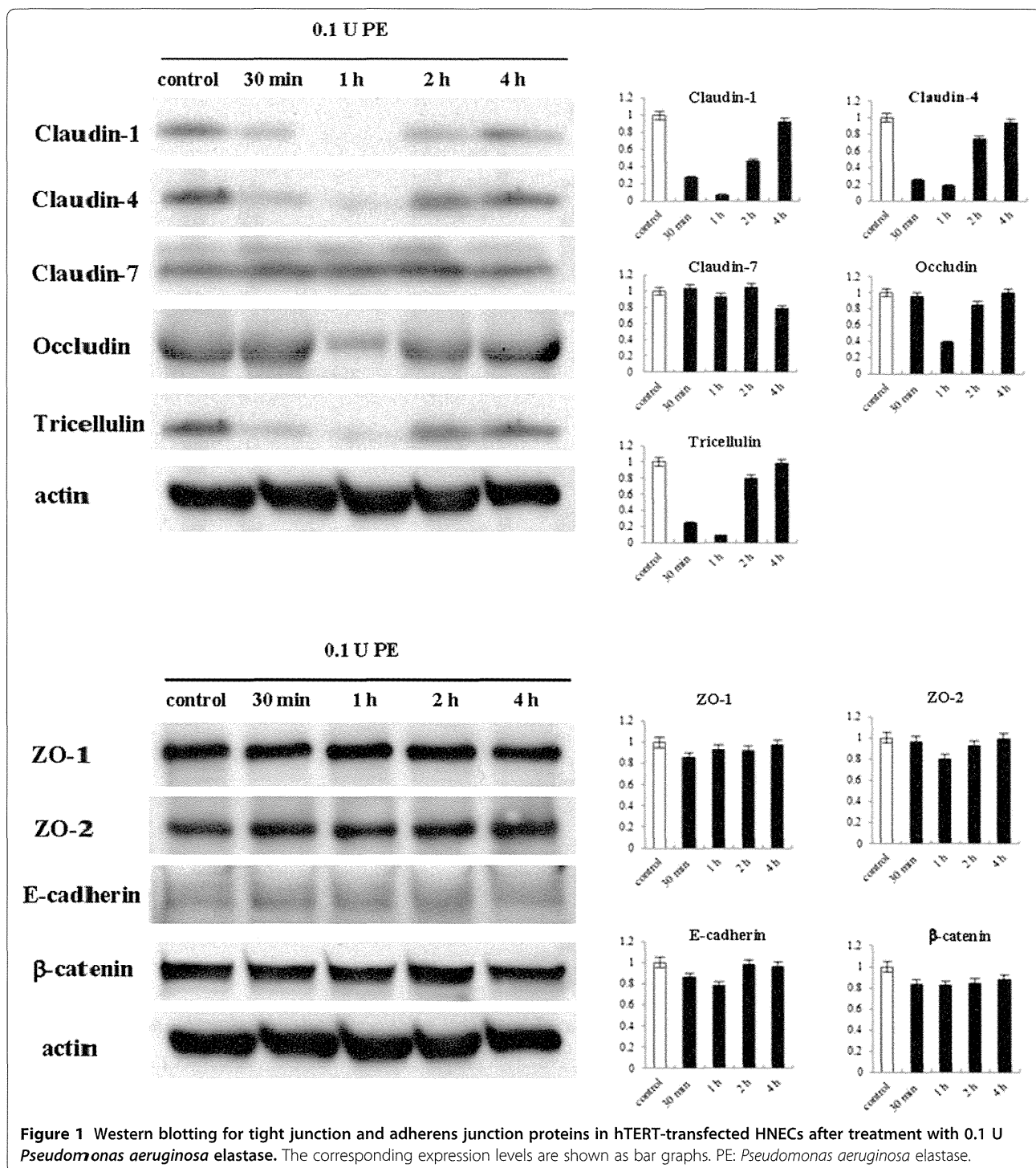
Data analysis

Signals were quantified using Scion Image Beta 4.02 Win (Scion Co.; Frederick, MA). Each set of results shown is representative of at least three separate experiments. Results are given as means ± SEM. Differences between groups were tested by ANOVA followed by a *post-hoc* test and an unpaired two-tailed Student's *t* test and considered to be significant when $p < 0.05$.

Results

P. aeruginosa elastase (PE) transiently reduces the expression of transmembrane proteins in the tight junctions in HNECs

To investigate whether *Pseudomonas aeruginosa* elastase (PE) affects the protein and mRNAs expression of tight junction and adherens junction molecules in HNECs, hTERT-HNECs were treated with 0.1 U PE for 30 min, 1 h, 2 h, and 4 h. Western blots showed that claudin-1, -4, and tricellulin protein levels decreased at 30 min but were restored at 2 h, whereas occludin protein was transiently reduced at 1 h (Figure 1). No changes in claudin-7, ZO-1, ZO-2, E-cadherin, and β-catenin protein levels were observed post-treatment (Figure 1). The mRNA levels of claudin-1, -4, occludin, and tricellulin decreased at 30 min and were restored at 2 h, whereas claudin-7 mRNA level was slightly reduced from 30 min until 2 h (Figure 2).

Furthermore, we investigated the effects of neutrophil elastase (NE) on the expression of tight junction and adherens junction molecules in HNECs, to compare the effects of PE. When hTERT-HNECs were treated with

Table 2 Antibodies

Antibody	Type	Dilution		Company
		IS	WB	
claudin-1	pAb	1:100	1:1000	Zymed Laboratories (San Francisco, CA)
claudin-4	pAb		1:1000	Zymed Laboratories (San Francisco, CA)
claudin-7	pAb		1:1000	Zymed Laboratories (San Francisco, CA)
occludin	pAb	1:100	1:1000	Zymed Laboratories (San Francisco, CA)
tricellulin	pAb		1:1000	Zymed Laboratories (San Francisco, CA)
ZO-1	pAb		1:1000	Zymed Laboratories (San Francisco, CA)
ZO-2	pAb		1:1000	Zymed Laboratories (San Francisco, CA)
actin	pAb		1:1000	Sigma-Aldrich (St. Louis, MO)
E-cadherin	mAb (36)		1:2000	BD Biosciences (San Jose, CA)
β-catenin	pAb		1:1000	Zymed Laboratories (San Francisco, CA)

pAb; rabbit polyclonal antibody, mAb; mouse monoclonal antibody, IS; immunostaining, WB; Western blotting.

Figure 1 Western blotting for tight junction and adherens junction proteins in hTERT-transfected HNECs after treatment with 0.1 U *Pseudomonas aeruginosa* elastase. The corresponding expression levels are shown as bar graphs. PE: *Pseudomonas aeruginosa* elastase.

0.01 U NE for 30 min, 1 h, 2 h, and 4 h, claudin-1, occludin, and tricellulin protein levels were transiently reduced 30 min post-treatment with NE, while no changes in claudin-4, -7, ZO-1, ZO-2, E-cadherin and β-catenin protein levels were observed (Additional file 1). NE did not affect mRNA levels of claudin-1, occludin, and tricellulin (Additional file 1).

PE affects the distribution of transmembrane tight junction proteins and the formation of tight junction strands in HNECs

We investigated changes in the distribution of tight junction proteins in hTERT-HNECs 1 h, 2 h, and 4 h post-treatment with 0.1 U PE. In the control cells (0 h), strong immunoreactivity of occludin and claudin-1 was
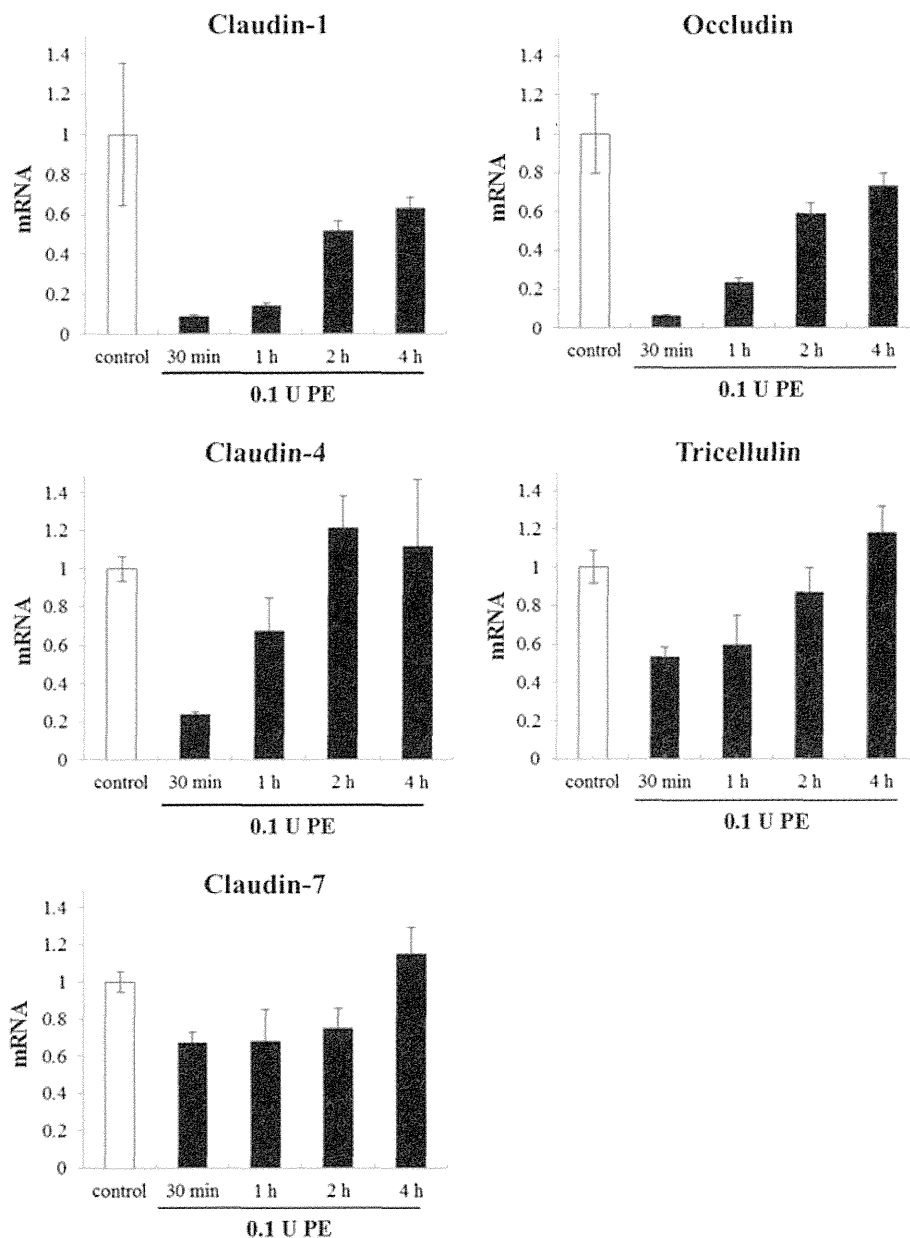
Figure 2 Real-time PCR analysis of claudin-1, -4, and -7, occludin, and tricellulin mRNA in hTERT-transfected HNECs after treatment with 0.1 U *Pseudomonas aeruginosa* elastase. PE: *Pseudomonas aeruginosa* elastase.
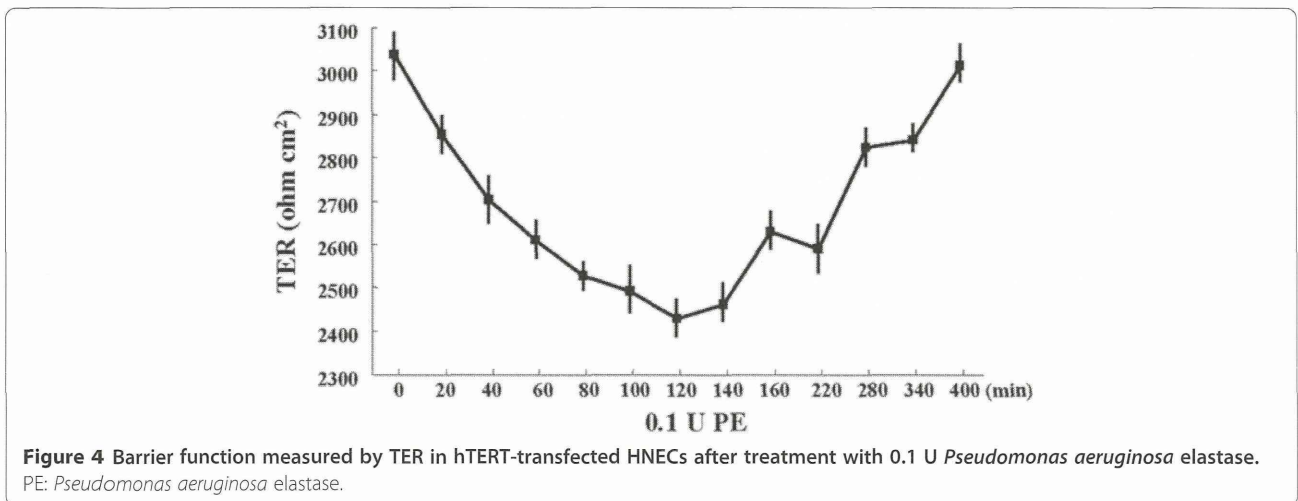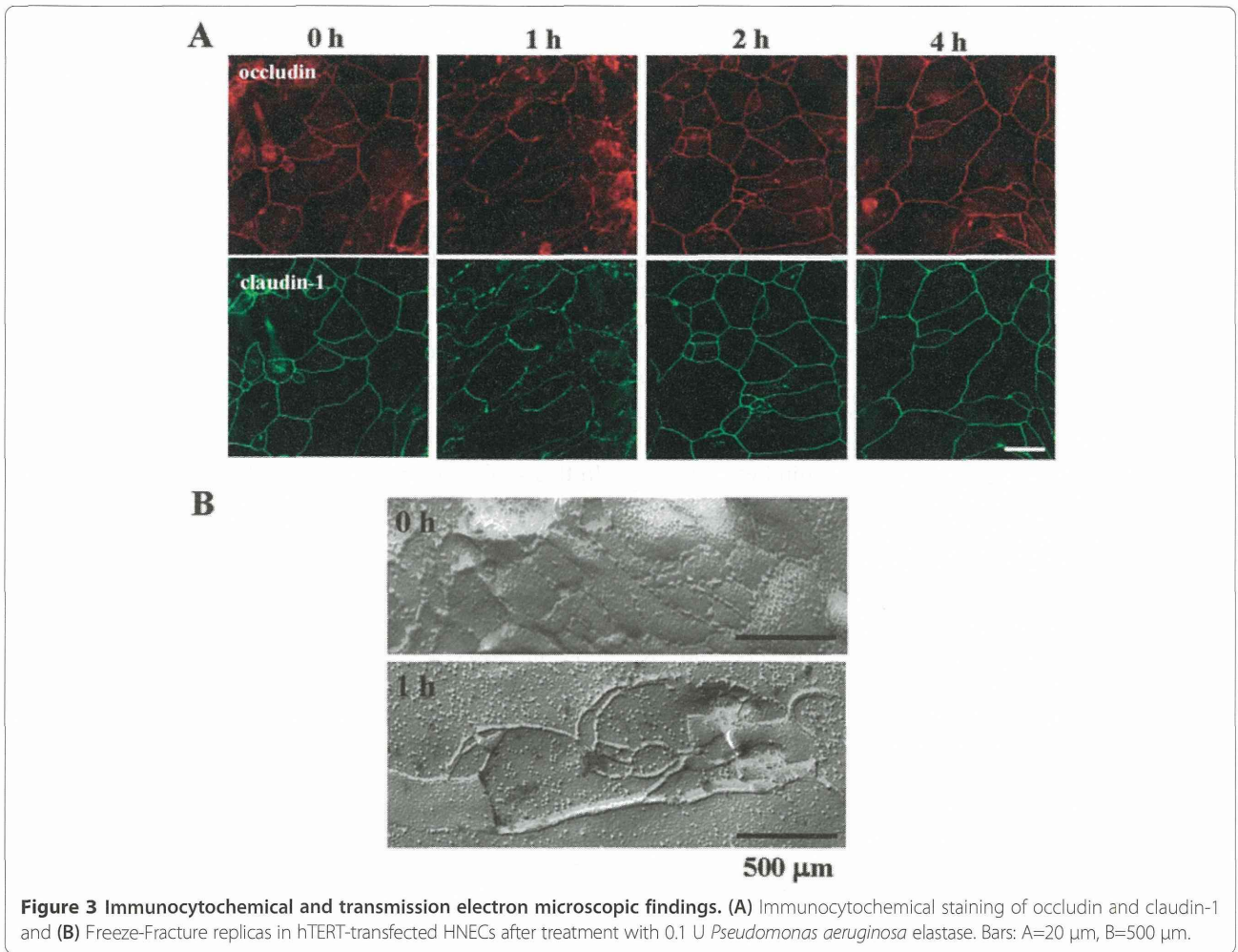
observed at the membranes (Figure 3A). The immuno-reactivities of occludin and claudin-1, in part, dis-appeared at the borders of some cells 1 h after treatment with PE and were then recovered 2 h post-treatment (Figure 3A).

Furthermore, we performed freeze-fracture analysis to investigate changes in the tight junction strands in hTERT-HNECs 1 h after treatment with 0.1 U of PE. In the control cells, a network composed of several continu-ous tight junction strands was observed (Figure 3B). The cells treated with PE exhibited a reduced number

of tight junction strands, which were partially disrupted (Figure 3B).

PE transiently reduces the tight junction barrier function of HNECs

To investigate the effects of PE on the tight junction barrier function of HNECs, hTERT-HNECs were treated with 0.1 U PE and then examined with continuous online measurements of transepithelial electric resistance (TER) by using a cellZscope. As shown in Figure 4, the TER was continuously decreased from 20 min to 120 min

Figure 3 **Immunocytochemical and transmission electron microscopic findings.** **(A)** Immunocytochemical staining of occludin and claudin-1 and **(B)** Freeze-Fracture replicas in hTERT-transfected HNECs after treatment with 0.1 U *Pseudomonas aeruginosa* elastase. Bars: A=20 μm, B=500 μm.

Figure 4 **Barrier function measured by TER in hTERT-transfected HNECs after treatment with 0.1 U** *Pseudomonas aeruginosa* **elastase.** PE: *Pseudomonas aeruginosa* elastase.

after PE-treatment, and continuously increased from 140 min to 400 min, recovering to the level prior to PE-treatment (Figure 4).

The reduction of transmembrane tight junction proteins by PE is regulated via distinct signaling pathway

It is reported that PE disrupts tight junctions via a PKC pathway (2). To investigate which signal transduction pathways affected the reduction of transmembrane tight junction proteins in HNECs after treatment with PE, hTERT-HNECs were pretreated with inhibitors of pan-PKC (GF109203X), MEK1/2 (U0126), PI3K (LY294002), p38 MAPK (SB203580), JNK (SP600125), EGFR (AG1478), COX1 (FR122047), COX2, NF-κB (IMD-0354), and Proteasome (MG132) at each 10 μg/ml 30 min before treatment with 0.1 U PE for 30 min or 1 h. The reduction of claudin-1 and occludin at 1 h after treatment with PE was prevented by GF109203X, U0126, LY294002, SP600125, inhibitors of COX1 and COX2, IMD-0354 and MG132 (Figure 5). The reduction of tricellulin at 1 h after treatment with PE was prevented by GF109203X, U0126, LY294002, and IMD-0354 (Figure 5). GF109203X, U0126, LY294002, SB203580, SP600125, and inhibitors of COX1 and COX2 inhibited claudin-4 reduction 30 min post PE treatment (Figure 5). No change of all tight junction proteins was observed at the concentrations of the various inhibitors without PE (Additional file 2).

PE reduces PAR-2 expression in HNECs

PE disables PAR-2 in airway epithelial cells A549 and 16 HBE cells (1). To investigate whether PE affects PAR-2 expression in HNECs, mRNA and protein in hTERT-HNECs 30 min, 1 h, 2 h, and 4 h after treatment with 0.1 U PE were examined by RT-PCR and Western blotting. PAR-2 but not PAR-1 mRNA was markedly decreased at 30 min and was restored at 2 h (Figure 6A). PAR-2 protein was transiently reduced 1 h after treatment (Figure 6B).

Knockdown of PAR-2 downregulates transmembrane tight junction proteins in HNECs with or without treatment with PE

We investigated whether PAR-2 expression affects transmembrane tight junction proteins in HNECs with or without treatment with PE. Occludin and claudin-1 mRNA and protein levels in hTERT-HNECs without PE-treatment were reduced by the knockdown of PAR-2 using siRNA (Figure 6C and D). The occludin and claudin-1 protein levels in hTERT-HNECs 1 h post treatment with 0.1 U PE decreased after the knockdown of PAR-2 (Figure 6E).

The downregulation of transmembrane tight junction proteins by PE treatment is prevented by PAR-2 agonist

We investigated whether PAR-2 agonist prevents the reduction of transmembrane tight junction proteins caused by PE treatment in HNECs. When hTERT-HNECs were pretreated with 10–200 μM PAR-2 agonist 30 min before treatment with 0.1 U PE for 1 h, disruption of occludin and claudin-1 at the membranes after PE treatment was prevented in cells that were treated with PAR-2 agonist concentrations of 100 μM or more (Figure 7A). The downregulation of occludin and claudin-1 mRNAs by PE was prevented by treatment with 100 μM of PAR-2 agonist (Figure 7B).

Discussion

In this study, we first found that PE transiently disrupted the epithelial barrier of HNECs by the downregulation of transmembrane tight junction proteins via distinct signal transduction pathways. Furthermore, PE decreased PAR-2 expression, which plays a crucial role in the maintenance of tight junction proteins in HNECs.

PE increases paracellular permeability in lung epithelial cells by causing tight junction disruption and cytoskeletal reorganization [6]. Furthermore, PE decreases epithelial barrier function in a time-dependent manner in the human bronchial adenocarcinoma cell line Calu-3 by reduced localization of occludin and ZO-1 in the membrane fraction [2]. In these airway epithelial cells, the barrier function is not recovered after treatment with PE. In the present study, treatment with PE transiently decreased the epithelial barrier of HNECs together with downregulation of the transmembrane proteins claudin-1 and -4, occludin, and tricellulin but not the scaffold PDZ-expression proteins ZO-1 and -2 and adherens junction proteins E-cadherin and β-catenin. Furthermore, reduced localization of occludin and claudin-1 and the disruption of tight junction structure were observed following PE treatment. Nevertheless the expression of claudin-1 and occludin by treatment with PE was markedly reduced at the level of mRNA and protein compared to the control, the immunostaining of these two proteins did not represent the dramatic reduction. In the present study using HNECs, it is possible that PE may strongly affect the synthesis of the tight junction proteins rather than the localization, although the detailed mechanisms are unclear. Treatment with NE also transiently decreased claudin-1, occludin, and tricellulin protein levels in HNECs. The sensitivity to PE in HNECs and other airway epithelial cells is different. PE, as a thermolysin-like metalloproteinase [30], may more strongly degrade the extracellular loops of transmembrane proteins in HNECs than other airway epithelial cells.

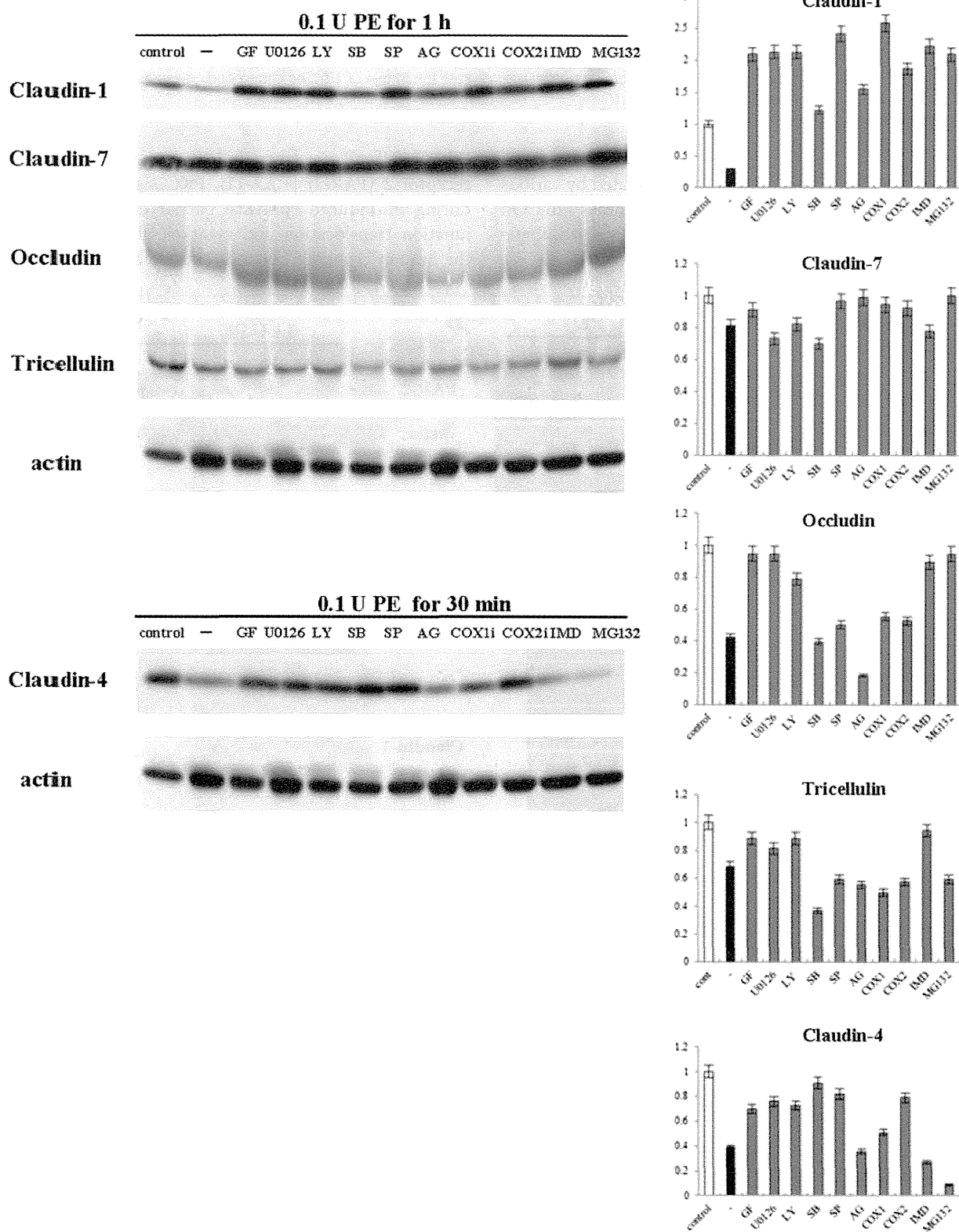The tight junction proteins are regulated by various cytokines and growth factors via distinct signal transduction

Figure 5 (See legend on next page.)

(See figure on previous page.)

Figure 5 Western blotting analysis. Western blotting for tight junction proteins in hTERT-transfected HNECs pretreatment with pan-PKC inhibitor (GF109203X), MEK1/2 inhibitor (U0126), PI3K inhibitor (LY294002), p38 MAPK inhibitor (SB203580), JNK inhibitor (SP600125), epidermal growth factor (EGF) receptor inhibitor (AG1478), COX1 inhibitor (FR122047), and COX2 inhibitor, NF-κB inhibitor (IMD-0354), and Proteasome inhibitor (MG132) before treatment with 0.1 U *Pseudomonas aeruginosa* elastase for 30 min or 1 h. The corresponding expression levels are shown as bar graphs. PE: *Pseudomonas aeruginosa* elastase.

pathways [23,31]. In HNECs *in vitro*, tight junction proteins and the barrier function are also regulated by various stimuli via distinct signal transduction pathways [25]. On the other hand, PE affects the epithelial cells via multiple mediators of signaling, including activation of PKC, EGFR, Erk1/2, NF-κB, urokinase/uPAR and protease activated receptor-2 (PAR-2) [1,2,7-11]. PKC signaling is involved during PE-induced epithelial barrier disruption via tight junction translocation and cytoskeletal reorganization in the human bronchial adenocarcinoma cell line Calu-3 [2].
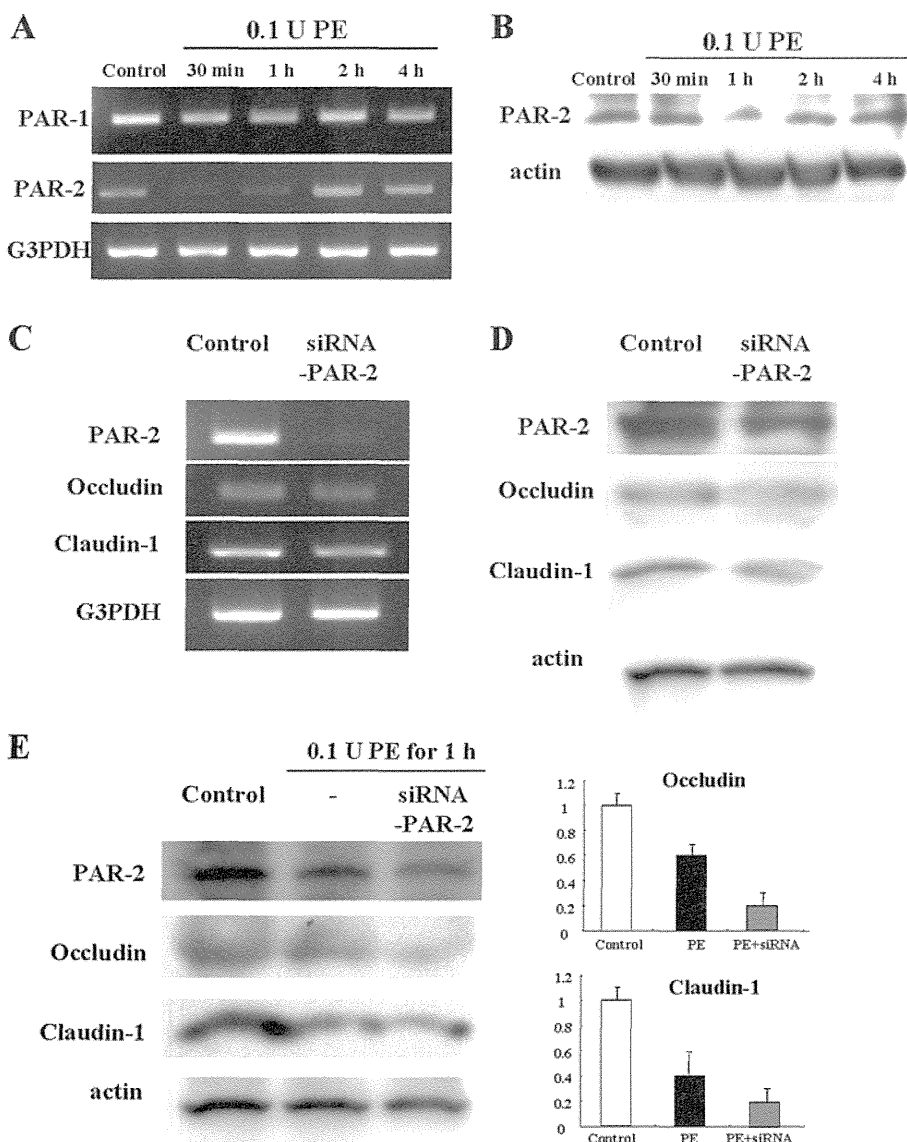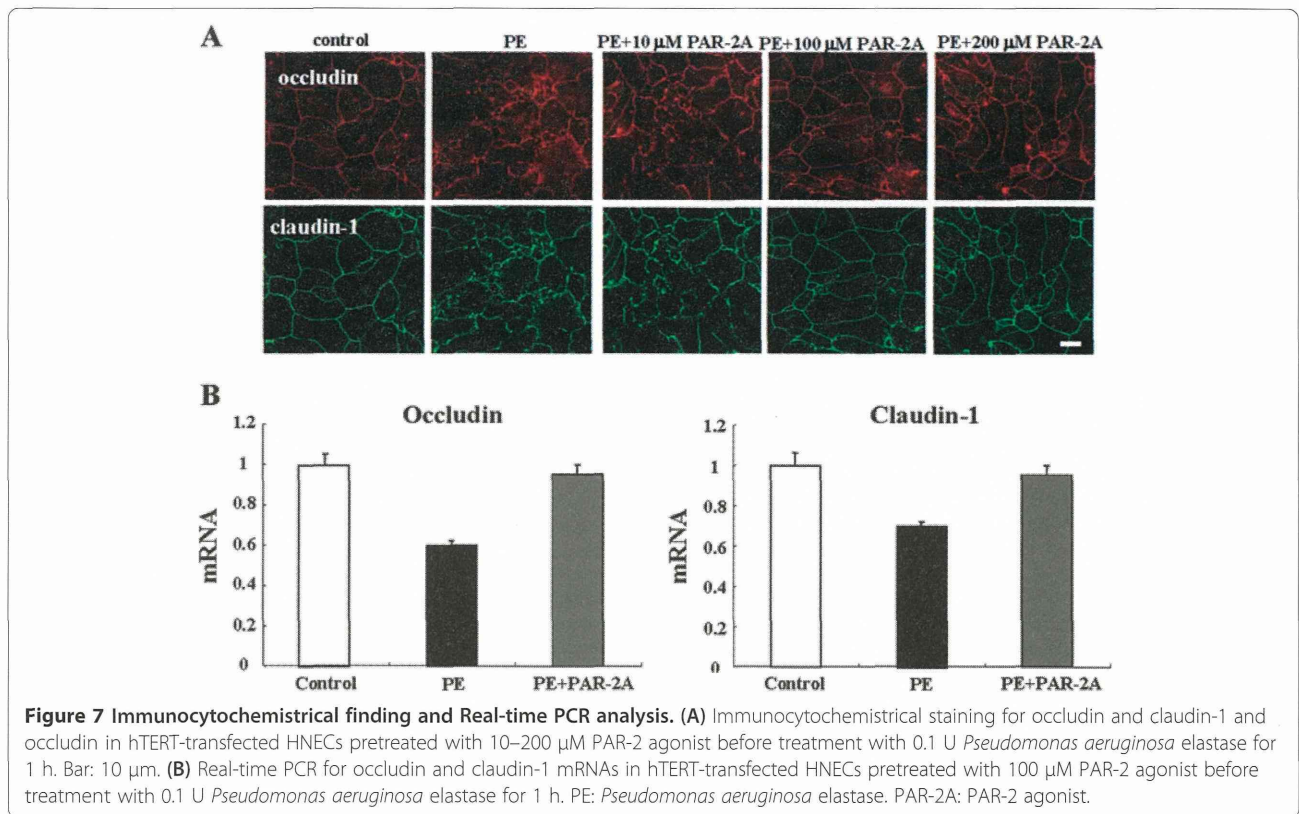

Figure 6 RT-PCR and Western blotting analyses. (A) RT-PCR for PAR-1 and -2 and **(B)** Western blotting for PAR-2 in hTERT-transfected HNECs after treatment with 0.1 U *Pseudomonas aeruginosa* elastase. **(C)** RT-PCR and **(D)** Western blotting for PAR-2, occludin, and claudin-1 in hTERT-transfected HNECs after treatment with siRNA of PAR-2 for 48 h. **(E)** Western blotting for PAR-2, occludin, and claudin-1 in hTERT-transfected HNECs pretreated with PAR-2 siRNA before treatment with 0.1 U *Pseudomonas aeruginosa* elastase for 1 h. The corresponding expression levels are shown as bar graphs. PE: *Pseudomonas aeruginosa* elastase.

Figure 7 Immunocytochemistrical finding and Real-time PCR analysis. (A) Immunocytochemistrical staining for occludin and claudin-1 and occludin in hTERT-transfected HNECs pretreated with 10–200 μM PAR-2 agonist before treatment with 0.1 U *Pseudomonas aeruginosa* elastase for 1 h. Bar: 10 μm. **(B)** Real-time PCR for occludin and claudin-1 mRNAs in hTERT-transfected HNECs pretreated with 100 μM PAR-2 agonist before treatment with 0.1 U *Pseudomonas aeruginosa* elastase for 1 h. PE: *Pseudomonas aeruginosa* elastase. PAR-2A: PAR-2 agonist.

In the present study of HNECs, the transient downregulation of the transmembrane tight junction proteins by treatment with PE was controlled via distinct signal transduction pathways such as PKC, MEK1/2, PI3K, p38 MAPK, JNK, COX-1, -2 and NF-κB. Furthermore, there are, in part, the different signal pathways among downregulation of the tight junction proteins by PE. Treatment with PE transiently downregulated mRNAs of the tight junction molecules in HNECs. These data suggest that PE rapidly induces the activation of multiple signaling mediators in HNECs and indirectly affects the synthesis of transmembrane tight junction proteins via distinct signaling pathways.

PE disables PAR-2 in A549 airway epithelial cells and in 16 HBE cells [1]. The activation of PAR-2 initiates multiple effects including enhanced airway inflammation and reactivity [13]. PAR-2 also affects the airway epithelial barrier [16]. In the present study, PE transiently reduced PAR-2 at mRNA and protein level in HNECs. Knockdown of PAR-2 using siRNA resulted in the downregulation of occludin and claudin-1 at the mRNA and protein levels. Furthermore, the knockdown of PAR-2 greatly enhanced the downregulation of occludin and claudin-1 by treatment with PE. It is thought that PAR-2 may play a crucial role in maintenance of tight junctions in HNECs. These data indicate that PE affects expression of tight junction proteins via PAR-2 in HNECs. We investigated whether

PAR-2 agonist prevents the reduction of transmembrane tight junction proteins by treatment with PE in HNECs. Treatment with more than 100 μM PAR-2 agonist could prevent delocalization of occludin and claudin-1 and downregulation of the mRNAs. However, in the present study, the knockdown of PAR-2 with siRNA did not affect the barrier function in the control HNECs (data not shown). Furthermore, when we measured TER in HNECs pretreated with a PAR-2 agonist before treatment with PE, a PAR-2 agonist did not protect the disruption of barrier function by PE (data not shown). These suggest that PAR-2 in part regulates the expression of tight junction proteins but not the barrier function in HNECs.

In conclusion, PE transiently disrupts tight junctions in HNECs through multiple effects: direct degradation, distinct signal transduction, and downregulation of PAR-2. *P. aeruginosa* is related to prolonged CRS [3]. The transient disruption of tight junctions may be repeatedly caused during CRS by PE and induce secondary infection by bacteria. PAR-2 agonists might be useful for the prevention and treatment of CRS.

Additional files

Additional file 1: (A) Western blotting for tight junction and adherens junction proteins in hTERT-transfected HNECs after treatment with 0.01 U neutrophil elastase. (B) RT-PCR for mRNAs of

tight junction molecules in hTERT-transfected HNECs after treatment with 0.01 U neutrophil elastase. NE: neutrophil elastase.

Additional file 2: Western blotting for tight junction proteins in hTERT-transfected HNECs treatment with pan-PKC inhibitor (GF109203X), MEK1/2 inhibitor (U0126), PI3K inhibitor (LY294002), p38 MAPK inhibitor (SB203580), JNK inhibitor (SP600125), epidermal growth factor (EGF) receptor inhibitor (AG1478), COX1 inhibitor (FR122047), and COX2 inhibitor, NF-κB inhibitor (IMD-0354), and Proteasome inhibitor (MG132) without *Pseudomonas aeruginosa* elastase.

Competing interests

The authors declare that they have no competing interest.

Authors' contributions

KN and TK carried out the genetic cell biological studies and drafted the manuscript. KO, RM and SH participated in cell culture. KT participated in the design of the study and performed the statistical analysis. TH and SN conceived of the study, and participated in its design and coordination and helped to draft the manuscript. All authors read and approved the final manuscript.

Author details

[1]Departments of Otolaryngology, Sapporo Medical University School of Medicine, Sapporo 060-8556, Japan. [2]Departments of Pathology, Sapporo Medical University School of Medicine, Sapporo 060-8556, Japan. [3]Departments of Pediatrics, Sapporo Medical University School of Medicine, Sapporo 060-8556, Japan. [4]Department of Cell Science, Research Institute for Frontier Medicine, Sapporo Medical University School of Medicine, South-1, West-17, Chuo-ku, Sapporo 060-8556, Japan.

References

1. Dulon S, Leduc D, Cottrell GS, D'Alayer J, Hansen KK, Bunnett NW, Hollenberg MD, Pidard D, Chignard M: Pseudomonas aeruginosa elastase disables proteinase-activated receptor 2 in respiratory epithelial cells. *Am J Respir Cell Mol Biol* 2005, 32:411–419.
2. Clark CA, Thomas LK, Azghani AO: Inhibition of protein kinase C attenuates Pseudomonas aeruginosa elastase-induced epithelial barrier disruption. *Am J Respir Cell Mol Biol* 2011, 45:1263–1271.
3. Ramakrishnan JB, Kingdom TT, Ramakrishnan VR: Allergic rhinitis and chronic rhinosinusitis: their impact on lower airways. *Immunol Allergy Clin North Am* 2013, 33:45–60.
4. Döring G, Goldstein W, Röll A, Schiøtz PO, Høiby N, Botzenhart K: Role of Pseudomonas aeruginosa exoenzymes in lung infections of patients with cystic fibrosis. *Infect Immun* 1985, 49:557–562.
5. Woods DE, Lam JS, Paranchych W, Speert DP, Campbell M, Godfrey AJ: Correlation of Pseudomonas aeruginosa virulence factors from clinical and environmental isolates with pathogenicity in the neutropenic mouse. *Can J Microbiol* 1997, 43:541–551.
6. Azghani AO, Miller EJ, Peterson BT: Virulence factors from Pseudomonas aeruginosa increase lung epithelial permeability. *Lung* 2000, 178:261–269.
7. Azghani AO, Baker JW, Shetty S, Miller EJ, Bhat GJ: Pseudomonas aeruginosa elastase stimulates ERK signaling pathway and enhances IL-8 production by alveolar epithelial cells in culture. *Inflamm Res* 2002, 51:506–510.
8. Leduc D, Beaufort N, de Bentzmann S, Rousselle JC, Namane A, Chignard M, Pidard D: The Pseudomonas aeruginosa LasB metalloproteinase regulates the human urokinase-type plasminogen activator receptor through domain-specific endoproteolysis. *Infect Immun* 2007, 75:3848–3858.
9. Beaufort N, Seweryn P, de Bentzmann S, Tang A, Kellermann J, Grebenchtchikov N, Schmitt M, Sommerhoff CP, Pidard D, Magdolen V: Activation of human pro-urokinase by unrelated proteases secreted by Pseudomonas aeruginosa. *Biochem J* 2010, 428:473–482.
10. Kida Y, Higashimoto Y, Inoue H, Shimizu T, Kuwano K: A novel secreted protease from Pseudomonas aeruginosa activates NF-kappaB through protease-activated receptors. *Cell Microbiol* 2008, 10:1491–1504.
11. Cosgrove S, Chotirmall SH, Greene CM, McElvaney NG: Pulmonary proteases in the cystic fibrosis lung induce interleukin 8 expression from bronchial epithelial cells via a heme/meprin/epidermal growth factor receptor/Toll-like receptor pathway. *J Biol Chem* 2011, 286:7692–7704.
12. Cocks TM, Fong B, Chow JM, Anderson GP, Frauman AG, Goldie RG, Henry PJ, Carr MJ, Hamilton JR, Moffatt JD: A protective role for protease-activated receptors in the airways. *Nature* 1999, 398:156–160.
13. Ebeling C, Forsythe P, Ng J, Gordon JR, Hollenberg M, Vliagoftis H: Proteinase-activated receptor 2 activation in the airways enhances antigen-mediated airway inflammation and airway hyperresponsiveness through different pathways. *J Allergy Clin Immunol* 2005, 115:623–630.
14. Knight DA, Lim S, Scaffidi AK, Roche N, Chung KF, Stewart GA, Thompson PJ: Protease-activated receptors in human airways: upregulation of PAR-2 in respiratory epithelium from patients with asthma. *J Allergy Clin Immunol* 2001, 108:797–803.
15. Yoshida T, Matsuwaki Y, Asaka D, Hama T, Otori N, Moriyama H: The expression of protease-activated receptors in chronic rhinosinusitis. *Int Arch Allergy Immunol* 2013, 161:138–146.
16. Yeoh S, Church M, Lackie P, McGill J, Mota M, Hossain P: Increased conjunctival expression of protease activated receptor 2 (PAR-2) in seasonal allergic conjunctivitis: a role for abnormal conjunctival epithelial permeability in disease pathogenesis? *Br J Ophthalmol* 2011, 95:1304–1308.
17. Takano K, Kojima T, Go M, Murata M, Ichimiya S, Himi T, Sawada N: HLA-DR- and CD11c-positive dendritic cells penetrate beyond well-developed epithelial tight junctions in human nasal mucosa of allergic rhinitis. *J Histochem Cytochem* 2005, 53:611–619.
18. Holgate ST: Epithelium dysfunction in asthma. *J Allergy Clin Immunol* 2007, 120:1233–1244.
19. Schleimer RP, Kato A, Kern R, Kuperman D, Avila PC: Epithelium: at the interface of innate and adaptive immune responses. *J Allergy Clin Immunol* 2007, 120:1279–1284.
20. Tsukita S, Furuse M, Itoh M: Multifunctional strands in tight junctions. *Nat Rev Mol Cell Biol* 2001, 2:285–293.
21. Sawada N, Murata M, Kikuchi K, Osanai M, Tobioka H, Kojima T, Chiba H: Tight junctions and human diseases. *Med Elecron Microsc* 2003, 36:147–156.
22. Schneeberger EE, Lynch RD: The tight junction: a multifunctional complex. *Am J Physiol Cell Physiol* 2004, 286:1213–1228.
23. Kojima T, Murata M, Yamamoto T, Lan M, Imamura M, Son S, Takano K, Yamaguchi H, Ito T, Tanaka S, Chiba H, Hirata K, Sawada N: Tight junction proteins and signal transduction pathways in hepatocytes. *Histol Histopathol* 2009, 24:1463–1472.
24. Ohkuni T, Kojima T, Ogasawara N, Masaki T, Ninomiya T, Kikuchi S, Go M, Takano K, Himi T, Sawada N: Expression and localization of tricellulin in human nasal epithelial cells in vivo and in vitro. *Med Mol Morphol* 2009, 42:204–211.
25. Kojima T, Go M, Takano K, Kurose M, Ohkuni T, Koizumi J, Kamekura R, Ogasawara N, Masaki T, Fuchimoto J, Obata K, Hirakawa S, Nomura K, Keira T, Miyata R, Fujii N, Tsutsumi H, Himi T, Sawada N: Regulation of tight junctions in upper airway epithelium. *Biomed Res Int* 2013, 2013:947072.
26. Kurose M, Kojima T, Koizumi JI, Kamekura R, Ninomiya T, Murata M, Ichimiya S, Osanai M, Chiba H, Himi T, Sawada N: Induction of claudins in passaged hTERT-transfected human nasal epithelial cells with an extended life span. *Cell Tissue Res* 2007, 330:63–74.
27. Koizumi J, Kojima T, Ogasawara N, Kamekura R, Kurose M, Go M, Harimaya A, Murata M, Osanai M, Chiba H, Himi T, Sawada N: Protein kinase C enhances tight junction barrier function of human nasal epithelial cells in primary culture by transcriptional regulation. *Mol Pharmacol* 2008, 74:432–442.
28. Ohkuni T, Kojima T, Ogasawara N, Masaki T, Fuchimoto J, Kamekura R, Koizumi JI, Ichimiya S, Murata M, Tanaka S, Himi T, Sawada N: Poly(I:C) reduces expression of JAM-A and induces secretion of IL-8 and TNF-α via distinct NF-κB pathways in human nasal epithelial cells. *Toxicol Appl Pharmacol* 2011, 250:29–38.
29. Obata K, Kojima T, Masaki T, Okabayashi T, Yokota S, Hirakawa S, Nomura K, Takasawa A, Murata M, Tanaka S, Fuchimoto J, Fujii N, Tsutsumi H, Himi T,

    Sawada N: Curcumin prevents replication of respiratory syncytial virus
    and the epithelial responses to it in human nasal epithelial cells.
    PLoS One 2013, 8:e70225.
30. Kooi C, Hodges RS, Sokol PA: Identification of neutralizing epitopes on
    Pseudomonas aeruginosa elastase and effects of cross-reactions on
    other thermolysin-like proteases. *Infect Immun* 1997, 65:472–477.
31. Gonzalez-Mariscal L, Hernández S, Vega J: Inventions designed to enhance
    drug delivery across epithelial and endothelial cells through the
    paracellular pathway. *Recent Pat Drug Deliv Formul* 2008, 2:145–176.

Neutralizing Antibody Against Granulocyte/Macrophage Colony–Stimulating Factor Inhibits Inflammatory Response in Experimental Otitis Media

Shin Kariya, MD, PhD; Mitsuhiro Okano, MD, PhD; Takaya Higaki, MD; Seiichiro Makihara, MD, PhD;
Takenori Haruna, MD; Motoharu Eguchi, MD, PhD; Kazunori Nishizaki, MD, PhD

Objectives/Hypothesis: Granulocyte/macrophage colony–stimulating factor is important in the pathogenesis of acute and chronic inflammatory disease. We hypothesized that granulocyte/macrophage colony–stimulating factor plays a pivotal role in middle ear inflammation and that neutralization of granulocyte/macrophage colony–stimulating factor would inhibit neutrophil migration into the middle ear and production of inflammatory mediators.

Study Design: Animal experiment.

Methods: We used transtympanic administration of lipopolysaccharide, a major component of gram-negative bacteria, into mice to induce an experimental otitis media. Control mice received injection of phosphate-buffered saline into the middle ear cavity. Mice were systemically treated with granulocyte/macrophage colony–stimulating factor neutralizing antibody or control immunoglobulin G via intraperitoneal injection 2 hours before transtympanic injection of lipopolysaccharide or phosphate-buffered saline. Middle ear effusions were collected. Concentrations of interleukin (IL)-1β, tumor necrosis factor (TNF)-α, keratinocyte chemoattractant, and macrophage inflammatory protein-2 in middle ear effusions were measured by enzyme-linked immunosorbent assay. Histologic examination of the middle ear was also performed.

Results: Transtympanic injection of lipopolysaccharide upregulated levels of granulocyte/macrophage colony–stimulating factor, IL-1β, TNF-α, keratinocyte chemoattractant, and macrophage inflammatory protein-2 in the middle ear. Concentrations of cytokines and chemokines were significantly decreased in mice injected with granulocyte/macrophage colony–stimulating factor neutralizing antibody. Infiltration of inflammatory cells into the middle ear cavity induced by lipopolysaccharide was also significantly reduced by neutralization of granulocyte/macrophage colony–stimulating factor.

Conclusions: Systemic injection of granulocyte/macrophage colony–stimulating factor neutralizing antibody inhibits the middle ear inflammation induced by lipopolysaccharide in mice. Our findings suggest that granulocyte/macrophage colony–stimulating factor may offer a novel therapeutic target for the management of intractable otitis media.

Key Words: Granulocyte/macrophage colony–stimulating factor, middle ear, otitis, cytokine, chemokine, lipopolysaccharide, endotoxin.

Laryngoscope, 123:1514–1518, 2013

INTRODUCTION

Otitis media is one of the most common diseases caused by infection with viral, bacterial, or fungal pathogens. Multiple factors affect the pathogenesis and pathophysiology of otitis media, including inflammatory mediators, Eustachian tube dysfunction, and pathogenicity of pathogens. Nasal inflammation resulting from allergic rhinitis or upper respiratory infection is also an important factor in the incidence of otitis media.[1] Numerous studies have also shown that cytokines and chemokines play key roles in the pathogenesis of otitis media.[2–4]

Granulocyte/macrophage colony–stimulating factor (GM-CSF) is first defined by its ability to generate in vitro colonies of mature myeloid cells from bone marrow–precursor cells and can promote the survival and activation of macrophages, neutrophils, and eosinophils, as well as maturation of dendritic cells. Recent studies have shown that GM-CSF and cytokines play principal roles in the immune system.[5] A few studies have examined the presence of GM-CSF in patients with otitis media with effusion, but the findings have not been consistent.[6–8]

Lipopolysaccharide (LPS), a component of the outer membrane in gram-negative bacteria, induces Toll-like receptor 4 signaling and is a potent inducer of